GIS Based Analysis of the Potential of Solar Energy of Roof Surfaces in Baton Rouge, Louisiana

by

Timothy Norbert Weyrer

2. Bachelor Thesis

Submitted in partial fulfillment of the requirement of the degree Bachelor of Science

Carinthia University of Applied Science
School of Geoinformation

Supervisors

Internal Supervisor: Dr. Gernot Paulus

School of Geoinformation, Carinthia University of Applied Sciences, Villach, Austria

External Supervisor: Dr. Michael Leitner

Department of Geography and Anthropology, Louisiana State University, Baton Rouge, Louisiana, USA

Baton Rouge, May 2011

Science Pledge

By my signature below, I certify that my thesis is entirely the result of my own work. I have cited all sources I have used in my thesis and I have always indicated their origin.

Villach, 09.06.2011

[Timothy Norbert WEYRER]

Acknowledgements

This thesis would not have been possible without the continuous support and understanding of my family and my closest friends. I owe my deepest gratitude to all of them.

I am deeply grateful to my external supervisor, Dr. Michael Leitner, Department of Geography and Anthropology, Louisiana State University, Baton Rouge, United States of America, who gave me the opportunity to do my internship at the Louisiana State University. His encouragement and his detailed and constructive comments guided me through the preparation of this thesis.

I would like to show my gratitude to my internal supervisor, Dr. Gernot Paulus, School of Geoinformation, Carinthia University of Applied Sciences, Villach, Austria, for his detailed review, constructive comments and for his excellent advice during the preparation of this thesis.

I want to offer my regards to the Austrian Marshall Plan Foundation for their financial support, which enabled me to undertake my research for my Bachelor Thesis at the Louisiana State University.

Finally, I would like to thank all other people who guided me through the preparation of this thesis.

Zusammenfassung

Diese Bachelorarbeit beschreibt die Entwicklung und Implementierung eines konzeptuellen Analyse Modells für die Berechnung des Solarpotentials von Hausdachflächen in Baton Rouge, Louisiana. Die Entwicklung des Modells ist in zwei Phasen unterteilt. Innerhalb der ersten Phase wird ein Basismodell erstellt und implementiert, welches zur Evaluierung des Berechnungsmodells verwendet wird. Es kann gezeigt werden, dass die berechneten Werte mit den Referenzwerten übereinstimmen. Es muss jedoch beachtet werden, dass das Berechnungsmodell nur für ein flaches Gebiet getestet worden ist. Es ist nicht bekannt, wie sich ein variierendes Geländeprofil auf die Qualität der Ergebnisse auswirkt. In der zweiten Phase wird das Basismodel weiterentwickelt, sodass das Solarpotential der Hausdachflächen bestimmt werden kann. Aufgrund einer zu ungenauen Datengrundlage werden zusätzlich zu den bestehenden Daten weitere Informationen zu den Hausdachflächen gesammelt und in die Analyse integriert. Weiters wird aufgrund von fehlenden Daten über den Baumbestand die Verschattung durch Bäume nicht in die Analyse mit einbezogen. Für die Verarbeitung der Daten sowie für die Berechnung der einfallenden Solarstrahlung wird GRASS GIS 6.4.1 verwendet. Um die Analysen zu beschleunigen und um ein semi-automatisches Verarbeiten der Daten zu ermöglichen, werden einzelne Workflows erstellt und mit Hilfe von UNIX Shell Scripts innerhalb von GRASS GIS implementiert. Das entwickelte konzeptionelle Modell wird am Beispiel von 50 ausgewählten Gebäuden des Campuses der Louisiana State University (LSU) umgesetzt. Separat wird für jedes Gebäude die vorhandene Dachfläche und die einfallende Solarstrahlung berechnet. Die Eignung der Dachflächen wird anhand eines Index beschrieben. Die durchschnittliche einfallende Solarstrahlung für die ausgewählten Gebäude beträgt 4.22 kWh/m^2 je Tag oder 1540.3 kWh/m^2, wenn man den Wert auf das ganze Jahr bezieht. Für die Berechnung des Energieertrags werden zwei verschiedene Arten von Solarzellen verwendet. Für die ausgewählten Gebäude wird somit ein jährliches Einsparungspotential von $1 - $1.5 Million bestimmt. Berechnet man auf Basis der erhaltenen Ergebnisse das Einsparungspotential für den gesamten LSU Campus,

wird ein Einsparungspotential von jährlich $5 - $7.5 Millionen prognostiziert. Die Kosten für die Anschaffung, Installation und Wartung der Solaranlagen sind nicht in den Prognosen enthalten.

Abstract

This thesis discusses the development and implementation of a conceptual model for the estimation of the solar potential of roof surfaces in Baton Rouge, Louisiana. The development of the model is divided into two steps. Within the first step a basic model is developed and implemented in order to evaluate the model of this research. The model produces accurate results for a study area with a flat topography. The influence of an uneven topographic profile was not tested in this project. In the second step the basic model is enhanced and adapted for the calculation of the solar potential of roof surfaces. Due to somewhat less accurate base data, additional information about roof surfaces is collected and included into the analysis. Another component not included in the analysis of roof surfaces is tree shadowing due to the lack of data about the tree coverage. For the processing of the data as well as for the calculation of the incoming solar irradiation GRASS GIS 6.4.1 is used. To speed up the analysis and to provide a semi-automated processing of the data, workflows are created and implemented using UNIX Shell scripts. GRASS GIS offers the possibility to execute these scripts. The final conceptual model is applied to 50 selected buildings of the Louisiana State University (LSU) main campus. For each of these 50 buildings the available roof surface area and the incoming solar irradiation are determined individually. The suitability of the roof surfaces is described through the suitability index. The average incoming solar irradiation for the selected buildings is 4.22 kWh/m2/day and 1540.3 kWh/m^2/year. Furthermore, two types of solar panels are selected to calculate the potential energy output. For the 50 selected buildings the potential energy output would be equivalent to $1 - $1.5 million. The total energy output for all buildings on the LSU Campus using solar irradiation would be equivalent to approximately $5 – $7.5 million. The purchase, the installation, and the maintenance of the solar panels are not included in the estimations made in this research.

Table of Contents

List of Abbreviations

CIAT	*International Center for Tropical Agriculture*
CPV	*concentrating photovoltaic*
CSP	*concentrating solar power*
DEM	*Digital Elevation Model*
DSM	*Digital Surface Model*
DTM	*Digital Terrain Model*
DOE	*U.S. Department of Energy*
ESRA	*European Solar Radiation Atlas*
ESRI	*Environmental Systems Research Institute*
FEMA	*Federal Emergency Management Agency*
GIS	*Geographic Information System*
GUI	*Graphical User Interface*
GRASS	*Geographic Resources Analysis Support System*
GRS 80	*Geodetic Reference System 1980*
GPS	*Global Positioning System*
IEA	*International Energy Agency*
IER	*Institute for Energy Research*
IMU	*Inertial Measurement Unit*
LDOTD	*Louisiana Department of Transportation and Development*
LiDAR	*Light Detection And Ranging*
LoD	*Level of Detail*
LSU	*Louisiana State University*
MAUP	*Modifiable Areal Unit Problem*
MESoR	*Management and Exploitation of Solar Resource Knowledge*
NAD 83	*North American Datum of 1983*
NASA	*National Aeronautics and Space Administration*
NAVD 88	*North American Datum of 1988*
RBT	*representative building topology*
PV	*photovoltaic*
PVGIS	*Photovoltaic Geographic Information System*
QGIS	*Quantum GIS*
SAGA	*System for Automated Geoscientific Analyses*
SBDART	*Santa Barbara DISORT Atmospheric Radiation Transfer*
SRTM	*Shuttle Radar Topography Mission*
SEGS	*solar electric generation systems*
SHC	*Solar Cooling & Cooling Programme*
USACE	*U.S. Army Corps of Engineers*
USGS	*U.S. Geological Survey*
WGS84	*World Geodetic Survey System of 1984*
W/m^2	*watts per square meter*
Wh/m^2	*watt-hours per square meter*

1. Introduction

In the following Sub-Sections the main content of this research is described. It starts with a delineation of the motivation. Then the goal and the expected results of this research are described. Furthermore, a hypothesis is established and an overview about the structure of this work is given.

1.1 Motivation

Today people are faced with increasing gasoline prices, human-induced disasters, such as the oil catastrophe in the Gulf of Mexico in April 2010, or the nuclear catastrophe in Japan after the earthquake in March 2011. At the end of February 2011 the second largest one-week increase in gasoline prices since 1990 occurred. Only during hurricane Katrina a higher one-week increase was documented (EIA, 2011). These are reasons for an increasing attention on the use of alternatives such as renewable energy. This research is focused on solar energy.

In 2008, renewable energy amounted to 7% of the total U.S. energy consumption. Only one percent of the renewable energy is taken in by solar energy. Petroleum (37%), natural gas (24%) and coal (23%) accounts for most of the total U.S. energy consumption (EIA, 2010).Worldwide the U.S. ranks 9th in the total numbers of installed solar collectors, behind countries such as China, Turkey, Germany or Austria (Weiss and Mauthner, 2010). The solar energy sector in the U.S. thus offers a huge potential as an important renewable energy source. Currently, the annual increase in photovoltaic (PV) production is about 50% with a continued decrease in costs. In 2008 the installation of a PV system cost $4 per Watt ($4/W), in contrast in 2015 proposed costs are estimated to be $2/W. A significant decrease in costs is most likely to continue (Fthenakis et al., 2009). Initiatives, such as the Solar America Cities program of the U.S. Department of Energy (DOE) are encouraging to speed up the use of solar technologies in the U.S.. Existing solutions have already

been implemented in cities such as Boston (Solar Boston Interactive GIS Map, 2007) or San Francisco (San Francisco Solar Map, 2007), where maps including the solar potential of buildings have been created for the public.

Motivated by increasing gasoline prices, decreasing costs for PV installations, and the high potential of the solar energy sector, this research aims to provide a discussion whether or not it would make sense for Baton Rouge´s inhabitants to install solar panels in their homes. Similar to the initiatives discussed above, it is hoped that this research will speed up the implementation of PV installations and the use of “free” solar energy by the inhabitants of Baton Rouge.

1.2 Goal of Work

The goal of this research is the evaluation of the potential for collecting solar power from roof surfaces of single buildings in Baton Rouge, Louisiana. Roof surfaces in selected parts of the study area will be evaluated about how much of the incoming solar irradiation it can capture. Evaluations are based on Light Detection And Ranging (LiDAR) data. In order to achieve this goal a conceptual analysis model for the calculation of incoming solar irradiance will be developed and implemented using an integrated calculation model in a Geographic Information System (GIS). The accuracy of the chosen model will be evaluated using collected reference values from weather stations. The model will be implemented for the East Baton Rouge Parish, using Digital Elevation Models (DEM) with different resolutions. Additionally, the influence of the Modifiable Areal Unit Problem (MAUP) on the results will be analyzed. Furthermore, for a better human understanding of the roofs aptitude it is planned to develop a “suitability-index” describing the suitability of roof surfaces utilizing the solar potential.

1.3 Expected Results

The expected results of this research are:

- Developing a conceptual analysis model for the calculation of the solar potential of roof surfaces.
- The evaluation of existing geodata regarding data quality and “fitness for use”.
- The implementation of the conceptual analysis model using Open Source GIS tools based on LiDAR data for Baton Rouge, Louisiana.
- The development and application of an index that describes the suitability of roof surfaces.

1.4 Hypothesis

Through the application of selected GIS integrated models, it is possible to estimate accurate values of incoming solar irradiation. Furthermore, GISs enable the aggregation of solar irradiation values to pre-defined areas such as footprints of houses.

1.5 Structure of Work

Section 2 describes the basic concepts of this thesis. It includes the description of the terminology as well as examples of existing solutions concerning solar energy. Section 3 discusses the methodology of this thesis, including the problem definition and the proposed method of solution. Furthermore, the study area and the data to be used are described in Section 3. This section concludes with a summary. In

Section 4 the results of this research are presented and discussed. It is followed by a discussion in Section 5 and a summary and future outlook in Section 6. Section 7 lists all references used in this research. Finally, the last two Sections include a list of figures and a list of tables.

2. Theoretical Background

To understand the context of this paper a detailed description of the basic concepts is given through this Section. First the types of solar radiation, then a calculation model for estimating the solar potential and shadowing are described. Furthermore an overview on solar systems, Light Detection And Ranging (LiDAR), Digital Elevation Models (DEM), Modifiable Areal Unit Problem (MAUP) and existing literature is given.

2.1 Solar Radiation

An enormous amount of solar radiation from the sun reaches the earth´s atmosphere every day. To cover the distance of 150 million kilometers (~93 million miles) the solar radiation needs 913 minutes (Ramachandra and Shruthi, 2007). This type of solar radiation is named extraterrestrial radiation with an average global irradiance of 1367 watts per square meter (W/m^2) (Noorian et al., 2008; Šúri and Hofierka, 2004). A large portion of the extraterrestrial radiation never reaches the earth´s surface, caused by absorption and scattering while passing through the atmosphere. Almost 30% of it is reflected and clouds, dust and gas absorb another 20%. Examples for gases are water vapor, carbon dioxide and ozone (Ramachandra and Shruthi, 2007).

The amount of solar radiation left is named global radiation (Klärle et al., 2009). It consists of direct- and diffuse radiation, whereby Pandey and Katiyar (2011) divide the diffuse radiation into sky diffuse and reflected diffuse radiation. Direct radiation passes the earth atmosphere unrestricted to the surface. The scattered radiation that reaches the surface is the sky diffuse radiation and the radiation reflected by the ground, mountains, water and buildings is the reflected diffuse radiation (see

Figure 1). Klärle et al. (2009), Noorian et al. (2008), Huld et al. (2003) and Šúri and Hofierka (2004) divide the global radiation in the following three components: direct-, diffuse- and reflected radiation. The reflected radiation is seen as an own component. This definition is applied in this paper. Rylatt et al. (2001) in turn divide global radiation only in direct- and diffuse radiation.

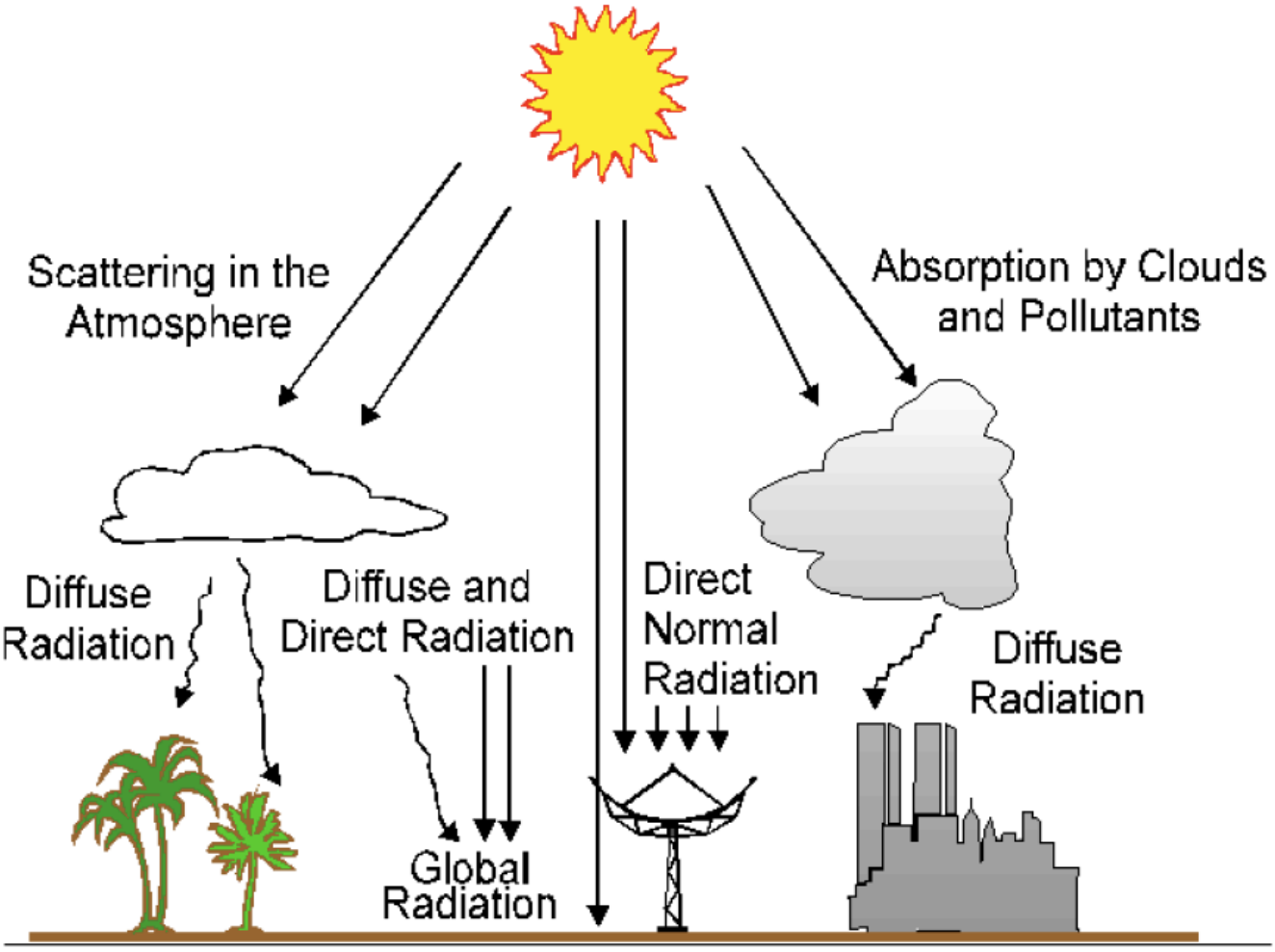

Figure 1 - Radiation flux of global radiation (Mesor, 2011)

The amount of solar radiation falling on a unit area per unit time (W/m^2) is called total solar irradiance. The term irradiation describes the total solar irradiance over a defined time interval in watt-hours per square meter (Wh/m^2) (Šúri and Hofierka,

2004).Both total solar irradiance and irradiation can be separated in a direct and diffuse component (Quaschning und Hanitsch, 1998).

2.2 Calculation Model

Within this Section a brief overview about the influential parameters for the calculation of the amount of solar radiation that reaches a surface (horizontal/inclined) per unit area is discussed. As one example, the calculation model of Chrysoulakis et al. (2004) is summarized below. The aim of them is the estimation of total solar irradiance (I_{Total}) at different time steps during the sunlight hours of the day using the SBDART (Santa Barbara DISORT Atmospheric Radiation Transfer) tool (SBDART MatLab Tool, 2011; SBDART Web Tool, 2011).

I_{Total} is calculated by summing up the direct irradiance (I_{Direct}) and the diffuse irradiance ($I_{Diffuse}$). For the calculation of both, the parameters x,y,z as coordinates, β representing the slope and θ as the angle of incidence have to be determined. θ is the angle between the normal to the surface and the sun-earth vector. For the calculation of θ the parameters surface azimuth angle (a), solar zenith angle (z_s) and the solar azimuth angle (a_s) have to be determined (see Figure 2).

β represents the variation in height within a raster cell (pixel) of the DEM, whereby the surrounding cells are included into the calculation. In general the slope is the variation in height over a specific distance and is denoted as value between 0 and 90 degrees. Angle a is the aspect/orientation of the inclined surface. It is described as the downslope direction of the pixel or specific distance and is given through a value between 0 and 360 degrees, starting at north and traversing clockwise. Therefore a value of 180 represents a downslope direction oriented to south. Both β and a can be estimated from the underlying DEM using GIS software solutions such

as ArcGIS (ArcGIS 2011) or GRASS (Geographic Resources Analysis Support System) GIS (GRASS GIS, 2011). Z_S is the angle between the direction of interest (sun-earth vector) and the normal to the horizontal plane. The last parameter $a_s$is described as the deviation between the sun-earth vector on the horizontal plane and the local meridian. All angles are given in degrees.

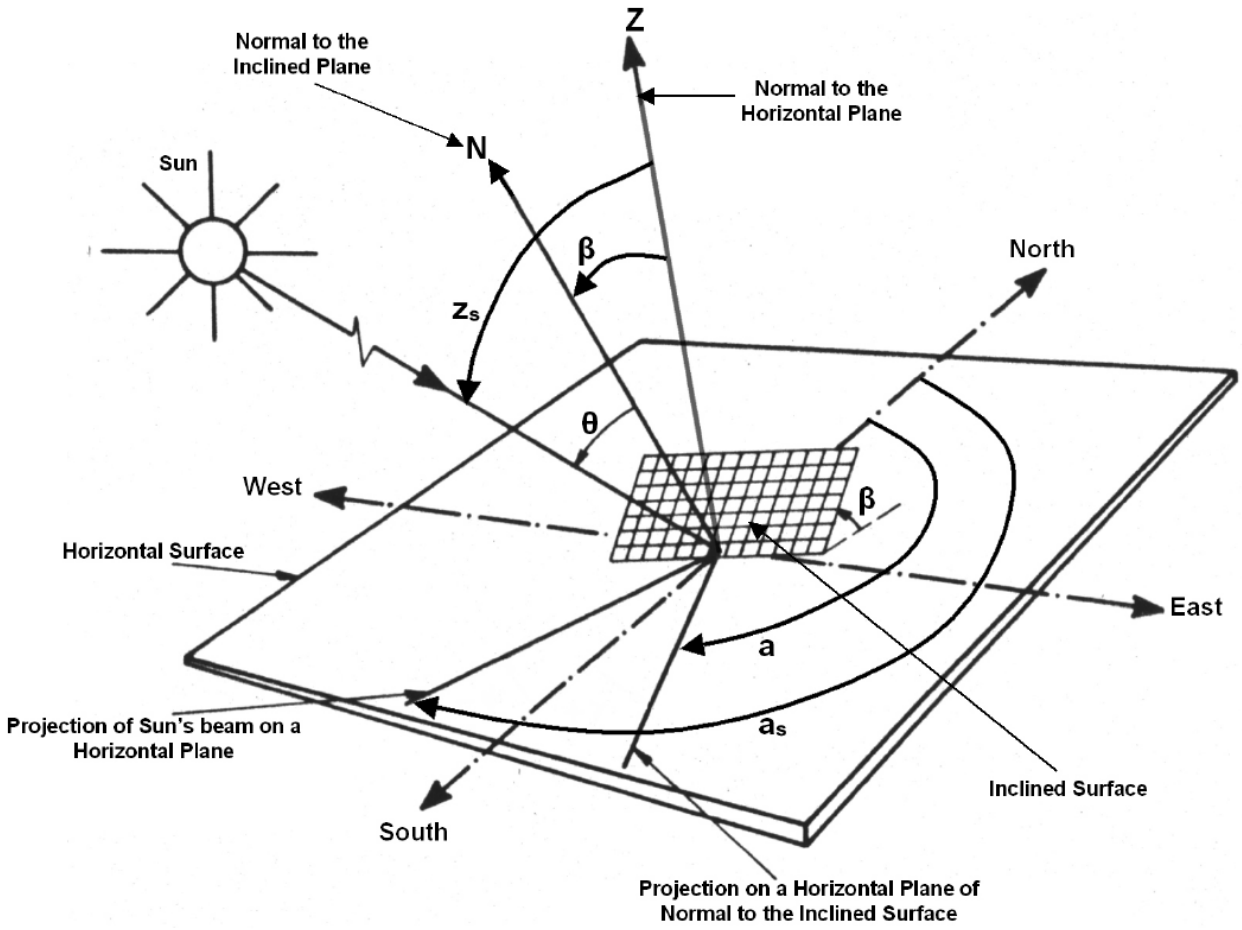

Figure 2 - The solar geometry described by Chrysoulakis et al. (2004)

Additionally, the model considers factors such as gas concentrations, cloud cover and surface albedo, but no further information about the integration of these factors is given. Moreover, this model does not consider the reflected diffuse irradiance. After determining all necessary parameters, I_{Direct} and $I_{Diffuse}$ can be estimated,

which in turn enables to compute of I_{Total} in W/m^2.Furthermore, the daily irradiation in kilowatt-hours per m2 (KWh/m^2) (E) is computed, using the time of measurement (t), the sunrise- (t_1) and sunset time (t_2). During a single day 85 measurements are taken by Chrysoulakis et al. (2004) and the average is taken to compute E.

Within the papers of Noorian et al. (2008) and Pandey and Katiyar (2011) different calculation models are compared and evaluated. In both papers it is recommended to use the calculation model of Skartveit and Olseth (1986). Moreover, Noorian et al. (2008) strongly recommend the calculation model of Perez et al. (1990). Due to their complexity the two models are out of the scope of this second Bachelor Thesis. In comparison, the model of Chrysoulakis et al. (2004) is a simplified version of the two models recommended in the literature.

2.3 Shading

A factor that influences the energy output of solar panels negatively is shading. When deciding whether to install a solar system or not, shading generated by objects such as trees, neighboring buildings, phone masts or chimneys have to be considered. By Levinson et al. (2009) divide shading into total- and extraparcel shading. Total shading is explained as shading caused by objects within the same study area. In contrast, objects outside of the study area cause extraparcel shading. The study area can be for example a rooftop. An object such as a chimney causes total shading. A tree causes extraparcel shading. Furthermore, the authors describe the reductions through shading by using the terms “light loss” and “light loss fraction”. If only diffuse solar irradiance is reaching the surface it is described as light loss. It is determined by forming the product of the shade fraction and the direct solar irradiance. The light loss fraction is the ratio of the light loss to global solar irradiance (Levinson et al., 2009). When deciding to install solar panels, it has

to be considered that shading in the morning and evening reduce energy output of solar panels less intensive (Kovach and Schmid, 1996).

2.4 Solar Systems

The two main types of solar panels are photovoltaic (PV) and thermal solar panels. PV panels directly convert the arriving solar radiation into electricity using the photoelectric effect/photovoltaic conversion (Parida et al., 2011; Sharma, 2011). In contrast thermal solar panels use the arriving solar radiation to generate thermal energy in form of heat. Moreover, it is stated that thermal solar panels are much less efficient and less expensive than PV solar panels (Herbst, 2009). In countries such as USA and Spain the generation of power through concentrating solar power (CSP) systems is quickly increasing (Klärle et al., 2009). CSP systems use mirrors and tracking systems to concentrate the arriving solar radiation on one point to generate thermal heat. It is used as heat source for conventional power plants. Examples for CSPs are the PS10 tower in Spain and 9 CSPs in California that belong to the solar electric generation systems (SEGS) project. SEGS represents the largest solar energy generating facility in the world. A method for generating electricity on a grand scale is concentrating PV (CPV). The same principle as in CSP systems is used and examples are the Sarnia PV power plant in Canada and the Strasskirchen Solar Park in Germany (Sharma, 2011).

Additionally to PV panels, Kovach and Schmid (1996) state that the orientation of the electrical connections is significant for the energy output. In case of vertical connections the output is higher due to lower electrical mismatching within the panels that is caused by shading.

2.5 Light Detection And Ranging (LiDAR)

LiDAR is defined as an airborne laser system that is fixed on board of an airplane in order to collect x-, y- and z-coordinates of the earth´s surface. It consists of the following three components: light-emitting scanning laser, high-precision Global Positioning System (GPS), and Inertial Measurement Unit (IMU). The system measures the distance between the scanning laser and the surface. The distance is determined by recording the time difference between the emission of the laser beam and the return of the reflected signal to the airplane. The high-precision GPS is responsible for determining the three dimensional positions of the sensor and the IMU for the measurement of the altitude of the system. After the flight the measurements of the three components are combined to generate the data points. In contrast to other airborne systems such as areal photogrammetry, LiDAR systems do not need daylight. LiDAR measurements can be done at night or on cloudy days. Nevertheless, weather conditions such as wind, snow and clouds should be avoided, because they reduce the accuracy of the output (FEMA, 2003).

2.6 Digital Elevation Model (DEM)

A DEM is a regularly raster in x and y direction that includes information about the altitude of the surface. Each raster cell includes one altitude value. DEMs are created using interpolation methods, applied for example on LiDAR data. The process of creating a raster out of LiDAR points entails that features such as ditches and buildings are not recognized, which, of course, is depending on the resolution of the resulting raster (FEMA, 2003). The term DEM is the hypernym for Digital Surface Model (DSM) and Digital Terrain Model (DTM). A DSM represents the surface including all objects. In contrast a DTM represents the surface excluding all objects.

2.7 Modifiable Areal Unit Problem (MAUP)

The MAUP is based on the fact that spatial units can be randomly determined and modified, in terms of aggregation and size. The MAUP is further divided into the scale- and aggregation problem. The scale problem is the variation in results that occur when data from one Level of Detail (LoD) are aggregated to another LoD. In contrast, the aggregation problem is the variation in results that appears through the choice of alternative spatial units, whereby the number of spatial units remains unchanged (Jelinski and Wu, 1996).

2.8 Literature Review

Due to the increased importance of renewable energy, especially in case of solar energy, many small- and large-scale projects have been introduced to estimate the solar potential. Furthermore, national and transnational initiatives were founded to support users and also those who are interested in using solar energy. Within this Literature Review an overview of these projects and initiatives is given.

2.8.1 Large-Scale Analysis

Large-scale projects are national and transnational (e.g., continental) projects that calculate solar potential for entire regions. Such large-scale solar potential analysis can be found for India (Ramachandra and Shruthi, 2007), Greece (Chrysoulakis et

al., 2004), Ontario (Nguyen and Pearce, 2010), and Europe (Šúri and Hofierka, 2004; Huld et al., 2003).

In Ramachandra and Shruthi (2007) the estimation of the potential of renewable energy (solar, wind, water, and biomass) is described for Karnataka, a state of India. Indirect methods are used for their calculations, when no data are available. The average monthly global solar radiation for the whole state of Karnataka is calculated and visualized on maps using a GIS. The values are estimated for 3 seasons, giving a range of values between 3.5 and 6.4 kWh/m^2. The slope and aspect (orientation) are not included in their calculations. Additionally, the difference between diffuse and direct radiation or shading are not taken into consideration in their study.

In contrast, the Chrysoulakis et al. (2004) model considers all the parameters that are not included in Ramachandra and Shruthi (2007). Using SBDART, the total solar irradiance for the city Heraklion, Greece is estimated. It is stated that the maximum solar irradiance is reached during midday, having values of 750 W/m^2. In the north of Heraklion a variability of ± 20 W/m^2 is given. Furthermore, it is noted that this study exhibits a rather poor accuracy for urban areas, because the DEM is not accurate enough.

The r.sun (Hofierka and Šúri, 2002) module is implemented in GRASS GIS (GRASS, 2011) and is used by Šúri and Hofierka (2004), Huld et al. (2003) and Nguyen and Pearce (2010) to estimate incoming solar radiation. The model is a result of the discussion in the ESRA (European Solar Radiation Atlas) project and is described in detail by Šúri and Hofierka (2004). It enables the calculation of global solar radiation and of each of its components (direct, diffuse, and reflected), by using the input parameters elevation above sea level, slope, aspect (all three are depending on the DEM), day number and local solar time. The day number is a value between 1 and 365, representing the day of the year. All other parameters are given or computed by the model itself. Furthermore, r.sun is described as a flexible and

efficient tool for estimating solar radiation for any atmospheric conditions (clear/cloudy sky). Solar radiation values are calculated for Central and Eastern Europe to determine the potential for PV systems. Finally, the results produced by r.sun are compared to stored data within the ESRA database. The ESRA database consists of solar irradiation data that are collected by 182 measurement stations. Especially during the period from October to April, the r.sun model is showing a better performance. Another important feature of the model is the consideration of shadowing (Šúri and Hofierka, 2004).

In order to provide decision makers, researchers, and industry with information about solar energy, the PVGIS website is introduced by Huld et al. (2003) for the 10 EU candidate states in 2003. For this reason a GIS database of solar radiation and PV potential estimations are realized. Using these data the annual potential in electricity generation is computed. The results are visualized on maps and provided to the public on the PVGIS website (Huld et al., 2003).

To identify suitable areas for installing PV farms in 14 counties of south-eastern Ontario the r.sun model is used (Nguyen and Pearce, 2010). Based on three criteria the study areas are selected. First, the study site has to be within 2km of an existing transmission line; second, it has to have at least 100 acres of land; and third, a slope lower than 4 degrees. For the suitable areas the solar potential is computed, giving an annual average of global irradiation of 3.57 kWh/m^2 per day. It is believed that these numbers are overestimated by 8.2% - 15.2%. However, it is stated that the suitable region could supply 60% of Ontario´s projected peak electricity demand in 2025.

To evaluate the influence of the accuracy of the underlying DEM on the calculations of the r.sun model, different resolutions (100m, 300m, 500m, 1000m, 3000 m) are used to estimate solar radiation(Cebecauer et al., 2007). A 100m DEM provides the most accurate solution. It is believed that a DEM resolution above 500m leads to an overestimation of solar radiation by up to 51%. Due to the large influence of the

resolution of the DEM on estimating solar radiation, it is recommended to select the resolution of the DEM carefully (Cebecauer et al. 2007).

2.8.2 Small Scale Analysis

The term small-scale projects represent projects for the calculation of solar potential of buildings and applied solar systems. Especially when determining the solar potential for buildings (rooftops, facades) surrounding objects that cause shading have to be considered. Examples for small-scale projects are given by Hofierka and Kanuk (2009), Izquierdo et al. (2008), Wiginton et al. (2010), Lehmann and Peter (2003), Compagnon (2004) and Klärle et al. (2009).

For the city Bardejov (Slovakia) a 3D building model, the r.sun model to calculate the incoming solar irradiance and PVGIS to estimate the PV output potential are used to determine the PV potential of rooftops (Hofierka and Kanuk, 2009).The buildings of the city are divided into four categories, including residential houses, blocks of flats, industrial areas, and other facilities (garages, schools, etc.). It is believed that the city could produce 45% of its electricity consumption by installing PV systems, although the study area covers only two thirds of the entire city. The most efficient buildings are blocks of flats, the least efficient are residential buildings. Within this project it is shown that the r.sun model estimations can also be used for urban areas (Hofierka and Kanuk, 2009).

Izquierdo et al. (2008) calculate the PV potential for rooftops in Spain based on a 90m DEM. The solar potential is divided into physical, geographic, and technical potential. The physical potential defines the amount of receiving solar irradiance. The geographic potential is represented by the available rooftops, and the technical potential is made up of the three aspects radiation (direct, diffuse, and reflected), shadow cast, and module PV efficiency. Using the representative building topology

(RBT) roof area estimations are calculated. The RBT is the ratio between the number of inhabitants or buildings and a specified surface area in km^2. These 16 different categorizations are characterized from L-L (low population density-low building density) to VH–VH (very high density -very high density). Based on this categorization available rooftops for PV installations are determined, giving a result of 571±183 km^2 (14±4.5 m^2/capita) of available roof area in Spain (Izquierdo et al., 2008). Based on this result of available roof areas and considering the economic factor the potential for solar hot water systems (SWHS) and PV systems is calculated by Izquierdo et al. (2011). After accounting for 70% of the hot water demand by installing SWHS, the remaining roof area can be used for PV installations. Using cost-supply curves defined by Izquierdo et al. (2010) the energy potential is arranged in increasing costs. In 70% of the municipalities only 20% of the roof area is needed to satisfy the demand of hot water, which in turn enables to additionally install a PV system. 5.5% of municipalities are found to be unsuitable for installing a SWHS. Throughout Spain 17% of available roof area is needed to serve70% of the hot water demand, leaving 83% suitable for PV installations.

A 5-step procedure for estimating the total rooftop PV potential of south eastern Ontario is developed by Wiginton et al. (2010). The first step of the procedure is the segmentation of the study in units. In step two 10 of these units are used as sample areas. Within these samples the roof areas are determined by using the Feature Analyst of ArcGIS (ArcGIS, 2011). Step 3 entails the extraction of the roof areas of the entire region, which enables to calculate the total roof area. The available rooftop area for PV installations is determined in step 4. Within the last step the total energy output is determined. Very similar to Izquierdo et al. (2008) a ratio between population density and roof area is established. For the whole study area an available roof are of 134±8.31 km^2 (70±4.34 m^2/capita) is estimated. If PV systems are installed on all available roof areas, 134% of the peak power demand is provided for this region (Wiginton et al., 2010).

Besides determining the available roof area for solar installations, the façade area is also evaluated for its potential for PV installations in 15 EU member states by Lehmann and Peter (2003). Based on the structural type and the regional data of Northrine-Westfalia (Germany) areas for PV installations are calculated. In total 7,000 km^2 (20.5 m^2/capita) are available for solar installations. Approximately 4,600 km^2 (13.4 m^2/capita) are roof areas and 2,400 km^2 (7.1 m^2/capita) are facade areas. Shadowing is considered with a factor of 0.9 for roofs and 0.66 for facades (Lehmann and Peter, 2003). The determination of the solar potential of façade areas is also considered by Compagnon (2004).

Based on LiDAR data, the solar potential for a test region in Los Angeles (Chile) is calculated by Klärle et al. (2008). In this example, the existing model (SUN AREA) is adapted to this region in Chile. Using irradiation, roof size, potential electricity generation, potential CO2 savings, power in KW and investment volume the solar energy potential is estimated. It is stated that 672 buildings, having a total roof area of 0.0461 km^2, are suitable for installing a solar power system.

Concluding this Sub-Section three examples of applied solar systems are briefly discussed. The first example integrates thermoelectric modules into conventional collectors that produce electricity in order to reduce heat within buildings (Maneewan et al., 2005). The second example represents a new roof design for domestic heating and cooling (Juanico, 2008). The final example deals with a comparison between PV cooling and solar thermal cooling in two different European cities (Hartmann et al., 2011).

2.8.3 Initiatives

In the past years a huge number of solar databases such as ESRA or PVGIS have been developed. Most of them use different approaches or calculates different

models. Because of this, there is uncertainty about data quality appears and it is difficult for the user to deal with this variety. To fix these problems the Management and Exploitation of Solar Resource Knowledge (MESoR) project was developed in 2007. Furthermore, the existing data are standardized to enable their application by the user without troubles (Mesor, 2011). Moreover, MESoR is connected to other initiatives such as the Solar Cooling & Cooling Programme (SHC) of the International Energy Agency (IEA) in case of SHC36. The so called Task 36 “Solar Resource Knowledge Management” aimed to support companies or organizations that deal with renewable energy. Information products to assist policymakers and project developers were provided to them. Participating countries were Austria, Canada, France, Germany, Spain, Switzerland, and the United States.SHC36 ended in June 2010 (IEA/SHC Task 36, 2010).An initiative of the U.S. Department of Energy (DOE) is named Solar America Cities program. In 2007 and 2008 25 cities were designated by the DOE to participate and represent the foundation of DOE´s Solar America Communities Program. The DOE provides financial and technical support to these cities to increase the use of solar energy. The cities have developed solar financing plans, shortened solar permitting processes and provide courses for solar installers. In April 2010, the DOE invested $10 million over 5 years to further promote the use of solar energy by two organizations in cities that are not actually part of the Solar America Cities program.

3. Methodology

This section presents the methodology of this thesis. At the beginning a problem definition is given. Then the two study areas are described, followed by a detailed description of the data being used. After the data description, the methodology of how the defined problems are solved is discussed. This includes the development of the conceptual analysis model, the implementation of the calculation model, and basic workflows for data processing. Finally, the Section is summarized.

3.1 Defining the Problem

Diverse GIS integrated calculation models can be found. Examples include: the "r.sun" (Hofierka and Šúri, 2002) module that is integrated into GRASS GIS (GRASS, 2011); the SAGA (System for Automated Geoscientific Analyses) GIS (SAGA, 2011) integrated modules "Incoming Solar Radiation" (Conrad, 2001) and "Insolation" (Conrad, 2006); and, "Area Solar Radiation" (ESRI, 2006) that is integrated into ArcGIS (ESRI, 2011). Each of these models uses different parameters and each of them needs further expert knowledge to understand and determine them. One challenge of this thesis was how to choose the calculation model and determine the associated parameters. Furthermore, it has to be considered that the GIS has to provide the functionality to prepare and process the data used. Unlike as it was expected, the needed accuracy of the LiDAR data is not given. Hence, objects that cause shading such as trees, chimneys or other buildings, the roofs slope and aspect cannot be derived from the LiDAR data. The determination of these parameters and the integration of them into the selected model represent additional challenges. The overall problem represents the development of a conceptual analysis model that encompasses all steps of this thesis in a logical and easy to understand.

3.2 Study Area

There are two study areas defined within this thesis. One study area is defined for the large-scale and one for the small-scale analysis. As mentioned in Sub-Section 1.2 it is necessary to evaluate the results of the chosen model. Due to this the study area for the large-scale analysis is the East Baton Rouge Parish (see Figure 3).It is located in the state of Louisiana (USA) and covers an area of approximately 1220 km^2 (471 square miles). Baton Rouge, the capital city of the state of Louisiana is located in East Baton Rouge Parish. According to the U.S. Census Bureau (2010) it has 434,633 inhabitants.

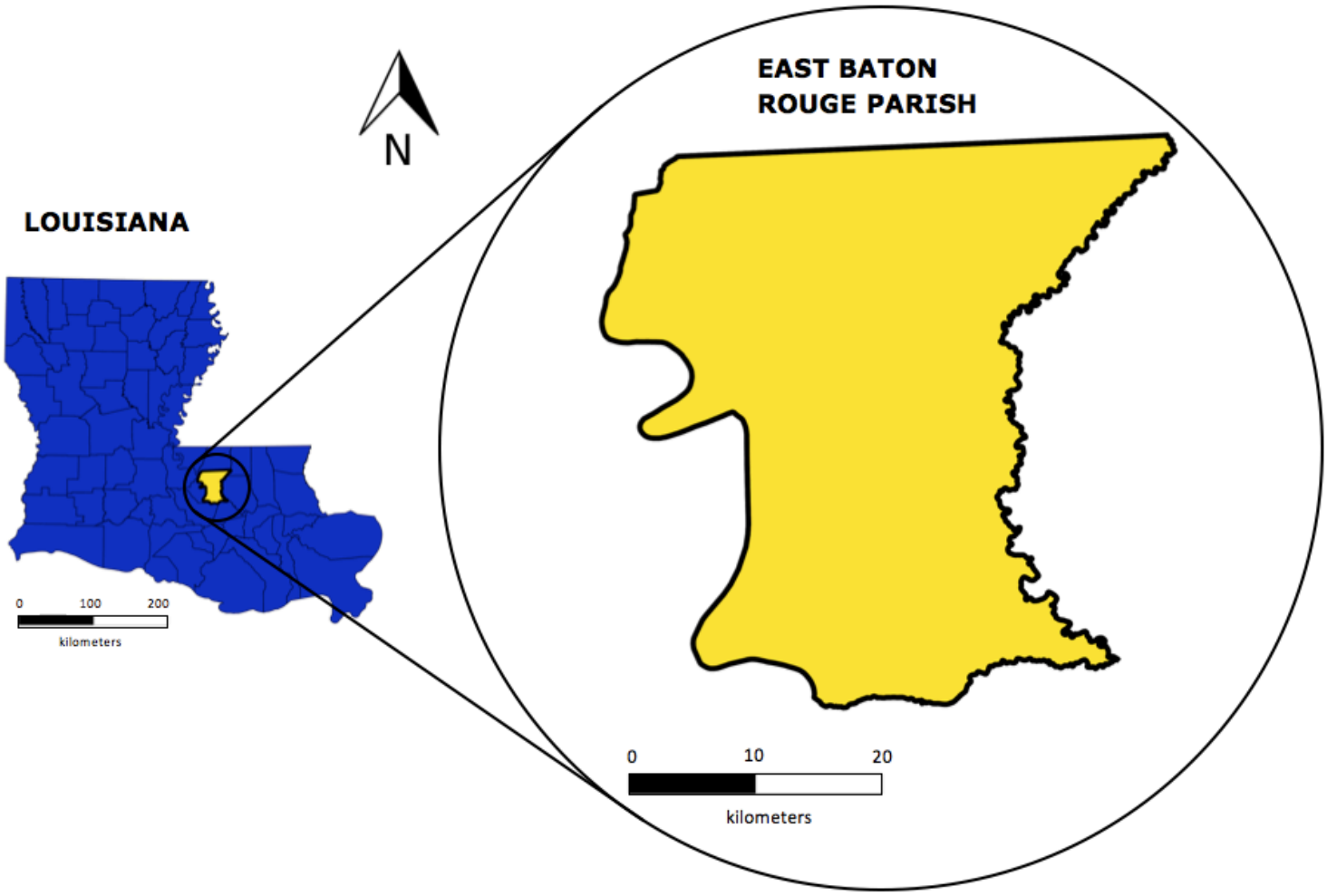

Figure 3–On the left the location of the study are within the state of Louisiana is shown. On the right the study area itself can be seen.

For the small-scale analysis the region of the main campus of the Louisiana State University (LSU) is chosen. It is located inside of the study area of the large-scale analysis (see Figure 4) and is situated in the south of Baton Rouge. There are more than 250 buildings on the main campus (LSU, 2011) and a representative number of them are selected for the solar potential analysis of the rooftops.

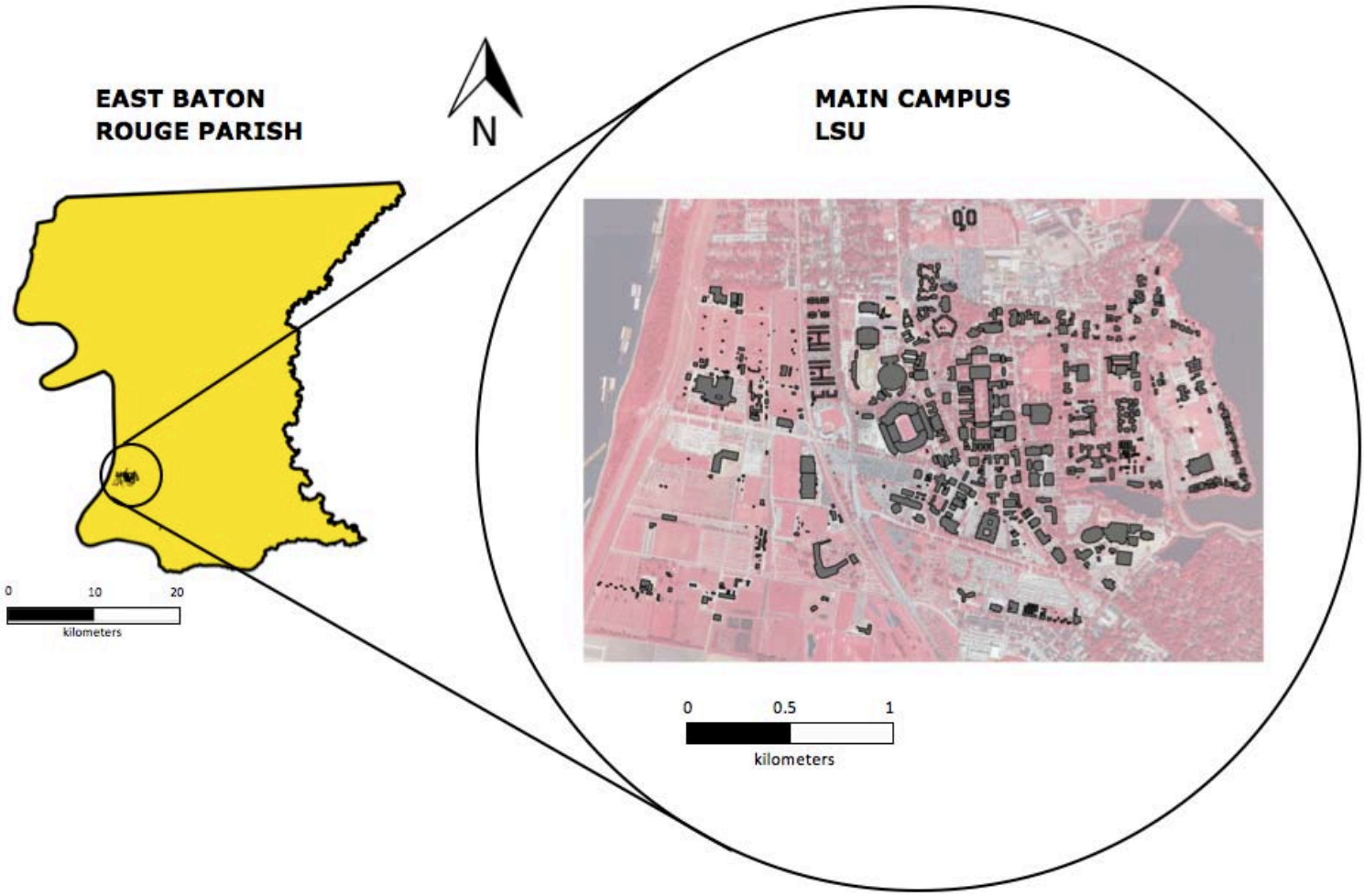

Figure 4–On the left the location of the small-scale study area inside of East Baton Rouge Parish can be seen. On the right the small-scale study area itself is shown.

3.3 Data

The data used in this research are classified into three categories. The first category of data is used for the large-scale analysis and can be seen in Table 1. The data of the second category are used for the small-scale analysis, where the roof surfaces are evaluated for their potential for collecting solar power (see Table 2). The third category of data is used for both types of analysis (see Table 3). This third category includes data sets that are needed for the calculating the model. All three tables within this Sub-Section include 5 columns. The first column includes an incremental

number and the second column the name of the dataset. The name comes undertaken from the metadata file or is chosen by the author. The third and the fourth columns include the file format and the file extension. Finally, the spatial representation of the data, raster or vector, is included in the fifth column.

Table 1–Data sets that are used for the large-scale analysis

	Data set name	File format	Extension	Spatial Representation
1	Global 30 Arc-Second Elevation (GTOPO 30)	Digital Elevation Model (DEM)	.dem	Raster
2	SRTM 90m Digital Elevation Database v4.1	Arc/Info ASCII Grid	.asc	Raster
3	1 Arc-Second National Elevation Dataset	GeoTIFF	.tif	Raster
4	Digital Elevation Model (USGS DEM), "*wx* " quadrant of "*yz*" quadrangle, Louisiana	Digital Elevation Model (DEM)	.dem	Raster
5	Louisiana Parish Boundaries	Shapefile	.shp	Vector

All data of category 1 (see Table 1) are open source and can be freely downloaded from the internet. Data sets 1-4 are all DEMs and they serve as input parameters for the model. Due to the testing of the influence of the MAUP on the results of the model, 4 different DEMs are chosen. The provider of dataset 1 is the U. S. Geological Survey (USGS). It is based on geographic coordinates (longitude/latitude in degrees) and is referenced to the World Geodetic Survey system of 1984 (WGS 84). It is described as a30 arc-second elevation dataset. This means that the horizontal resolution of this raster is approximately 1km. The altitude is given in meters, whereby no information about the accuracy has been provided (GTOPO30, 1996).

Data set 2 is provided by the International Center for Tropical Agriculture (CIAT). These data are derived from USGS/NASA (National Aeronautics and Space Administration) SRTM (Shuttle Radar Topography Mission) data through interpolation methods. Through this interpolation existing data voids are filled with values. It has the same projection and the same unit for measuring the altitude as data set 1 (e.g., meter). The horizontal resolution is approximately 90 meters and the average vertical error is reported to be less than 16 meters (Jarvis et al., 2008).

Similar to data set 1, data set 3 is also provided by the USGS and is based on stored DEMs of the USGS and its partners. It is expressed in geographic coordinates in conformance with the North American Datum of 1983 (NAD 83). The underlying ellipsoid is the Geodetic Reference System of 1980 (GRS 80) and the vertical datum is the North American Vertical Datum of 1988 (NAVD 88). The horizontal resolution is approximately 30 meters and the altitude values are described in meters. No additional information about the accuracy is given (USGS, 2009).

The last DEM, data set 4, is created by the U.S. Army Corps of Engineers (USACE), Saint Louis District and provided by LSU CADGIS Research Laboratory (2009). It is derived from LiDAR measurements that are created for terrain analysis and modeling. The projected coordinate system (x- and y-coordinate in meters) Universal Transverse Mercator (UTM), Zone 15 is used. The same horizontal/vertical datum and ellipsoid as in data set 3 are also used. The horizontal resolution is 5 meters. In contrast to the above mentioned datasets, altitude measurements are in feet. Unfortunately, no accuracy information is given (USACE 1, 2001).

The last data set in this category is used for determining the study area for the large-scale analysis. It is provided by the Louisiana Department of Transportation and Development (LDOTD) and is based on a manually digitized line network. The projection is the same as in data set 3, except that there is no need for a vertical datum, because there are no altitude values in this data set. A horizontal position accuracy of 40 feet (~12.2 meter) is provided (LDOTD, 2007).

Table 2–Data sets that are used for the small-scale analysis

	Data set name	File format	Extension	Spatial Representation
6	Building Footprints LSU Campus	Shapefile	.shp	Vector
7	Orthophoto LSU Campus	Joint Photographic Expert Group (JPEG) 200	.jp2	Raster
8	Raw LIDAR Elevation Data, NW quadrant of Baton Rouge West quadrangle, Louisiana	Comma Separated Value (CSV)	.csv	Vector
9	Aerial Campus Pictures	JPEG	.jpg	Raster

In Table 2 all data sets that are used for the small-scale analysis are listed. Data set 6 represents the building footprints of all buildings on the LSU campus. The footprints are manually digitized, using data set 7 as basis. It is expressed in projected coordinates. The underlying ellipsoid is the GRS 80, the horizontal datum is NAD 1983 and the horizontal units are given in feet. Data set 7 is created by the USGS and is provided by Atlas (2009). It has the same projection as data set 4. Displacements through sensor orientation and terrain relief are removed. Data set 7 has a horizontal resolution of 1 meter (USGS, 2004).

In contrast to the large-scale analysis that is based on free available DEMs, the small-scale analysis is based on free available LiDAR data (data set 8) that are in turn processed to a DEM. Data set 8 forms the basis for the small-scale analysis. It has the same creator, provider and projection as data set 4. The horizontal positional accuracy of the points is ±0.5 centimeters and the vertical accuracy is ±0.185 meters (USACE 2, 2001). Because there is no information about the point density of the LiDAR data, a representative subset is chosen to determine the point density. The result can be seen in Figure 5. It is created through overlaying the

subset on top of a 3x3 m raster. Results show that 42.72% (108496) of the cells do not include a point. Klärle et al. (2009) states that a point density of 2-3 points/m^2 is required to ensure that buildings, trees and other objects are recognized. Consequently, data set 6 does not fulfill the required point density that is needed for the analysis.

Category Information		%	cell
#	description	cover	count
0	. . . . .	42.72	108496
1	. . . . .	47.39	120361
2	. . . . .	9.30	23629
3	. . . . .	0.51	1299
4	. . . . .	0.06	157
5	. . . . .	0.01	23
6	. . . . .	0.00	5
TOTAL		100.00	253970

Figure 5 – Result of the statistic that is created through the overlay of the point subset and 3x3 m raster.

Due to the low point density, only the altitude information of data set 8 is used as input parameter for the model. The two parameters slope and aspect, that describe the inclination and orientation of the roof surface, are not derived from this data set. However, both parameters are essential for the estimation of the solar potential of roof surfaces. Consequently these parameters are collected “manually”. Furthermore, for the determination of the available roof surface, the roof type, the roof type coefficient, and the facility coefficient are also collected “manually”.

All roofs are classified into three categories:

- Gabled: The roof has a triangular form (see Figure 6 -left).
- Flat: The roof surface is flat (see Figure 6 – right)

Figure 6 – A gabled (left) and a flat (right) roof.

- Other: If a roof cannot be classified as either gabled or flat, it is classified as "Other". This encompasses all other possible roof types (see Figure 6). In this case, the roof surface can be divided into several sub-surfaces. Then, each sub-surface is evaluated separately.

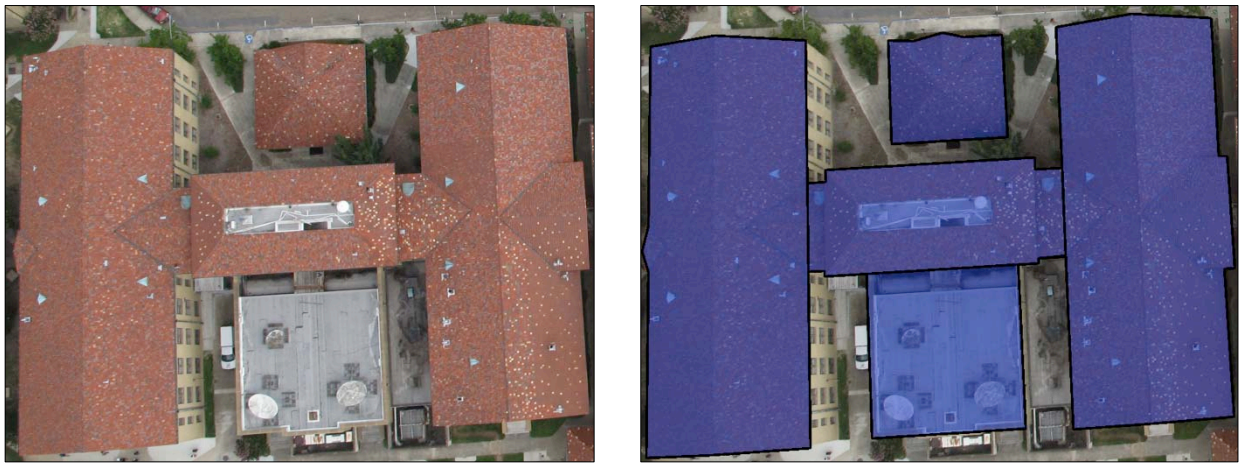

Figure 7 – A roof is shown that cannot be classified as gabled or flat (left). Dividing the same roof into sub-surfaces allows the evaluation of each individual sub-surface as either gabled or flat (right).

The roof type coefficient depends on the roof type. It describes the reduction of the roof surface that is caused by the roof type. The residual surface is named available roof surface (Izquierdo et al., 2008). A gabled roof has a roof type coefficient of 0.5 and a flat roof has a coefficient of 1. For other more complex roof types the roof type coefficient is determined after evaluation through the author. In general, the roof type coefficient can have values between 0 and 1.

The facility coefficient is a factor between 0 and 1 and describes how much of the available roof surface is occupied by other applications/objects such as chimneys or air conditioning systems (Izquierdo et al., 2008). A facility coefficient of 0 means that there is no space for solar panels left on the roof. In contrast, a coefficient of 1 means that there is no application/object on the roof that reduces the available roof surface.

The collected slope values are classified into the following 5 categories 0,10,20,30, and 40. For example a slope value of 30 means that the roof surfaces has an inclination of 30°. Based on this classification each roof surface is rated. The aspect values are classified into the 4 categories Null, South, South-West, and West. Levinson et al. (2009) described that most solar panels are installed on roofs that are oriented to the south, the south-west, or the west direction. If a roof has different orientation, it is rated as unsuitable and excluded from the analysis. The aspect is rated as “null”.

In order to determine the above mentioned parameters, a 3D-building model (GOSHEP, n.d.) and aerial pictures of the LSU campus (data set 9) are used. Furthermore, each object is directly observed by the author to re-check the selected parameter values.

Table 3 - These data sets are for both types of analysis

	Data set name	File format	Extension	Spatial Representation
10	Clearness Index	Text file	.txt	-
11	Albedo	Text file	.txt	-
12	Solar Reference Values	Text file	.txt	-

Data set 10, the clearness index, is used as a parameter for calculation of incoming solar irradiation. It describes the fraction of solar radiation that reaches the earth surface. It is defined as the ratio between the global- and extraterrestrial radiation. The ratio can have values between 0 and 1. The higher the value, the more solar radiation reaches the earth surface (Mellit et al., 2008). The dataset is provided by the National Renewable Energy Laboratory (NREL) (NREL 1, n.d.). Data set 11 describes the solar radiation that is reflected by the earth´s surface and serves as input parameter for the model. For this research one value (e.g. 0.16) is selected. This value was determined by Soule et al. (2006). The last data set includes monthly solar reference values that are selected to evaluate the results of the implemented model (NREL 2, n.d.; Gaisma, 2002).

3.4 Method of Solution

Within this Sub-Section the method of solution to the defined problems (see Sub-Section 3.1) is presented. Based on the offered functionality for processing data and the well-documented integrated r.sun module (Hofierka and Šúri, 2002) for the estimation of incoming solar irradiation, GRASS GIS 6.4.1 (GRASS, 2011) is selected for the data processing in this thesis. GRASS GIS is capable of using vector as well as raster data and offers more than 350 modules for the processing, management, analysis, and visualization of data. Furthermore, it supports the use

of more than 40 raster formats and offers the opportunity of script programming (UNIX Shell, Python, PERL) to automate workflows. The scripts can be “hard-coded” or the parameters can be defined when the script is invoked. Through the use of scripts a semi-automated processing of the data can be ensured (Neteler and Mitasova, 2008). For an easier interaction the GRASS GIS plug-in of Quantum GIS (QGIS) (QGIS, 2011) is used. QGIS provides the Graphical User Interface (GUI) and is used for the visualization of the data. Furthermore, QGIS is applied for digitizing purposes and modifications of the vectors attribute tables.

The development of the conceptual analysis model is divided into two steps. In the first step the model is developed and applied for the large-scale analysis, which is basically used for the evaluation of the results of the r.sun module. This step also includes the development of the selected model. Within the second step the model is further enhanced and adapted for the small-scale analysis, where the roof surfaces are evaluated on their solar potential.

This Sub-Section is further divided into two Sections. In the first the large-scale analysis and in the second the small-scale analyses is described.

3.4.1 Large-Scale Analysis

Because there is no information about the accuracy of the results of the selected model, a basic conceptual analysis model is developed to test the results (see Figure 8). This Sub-Section serves an overview about the model and describes the workflow from the data input to the results. It is organized in four components and each of them is described below.

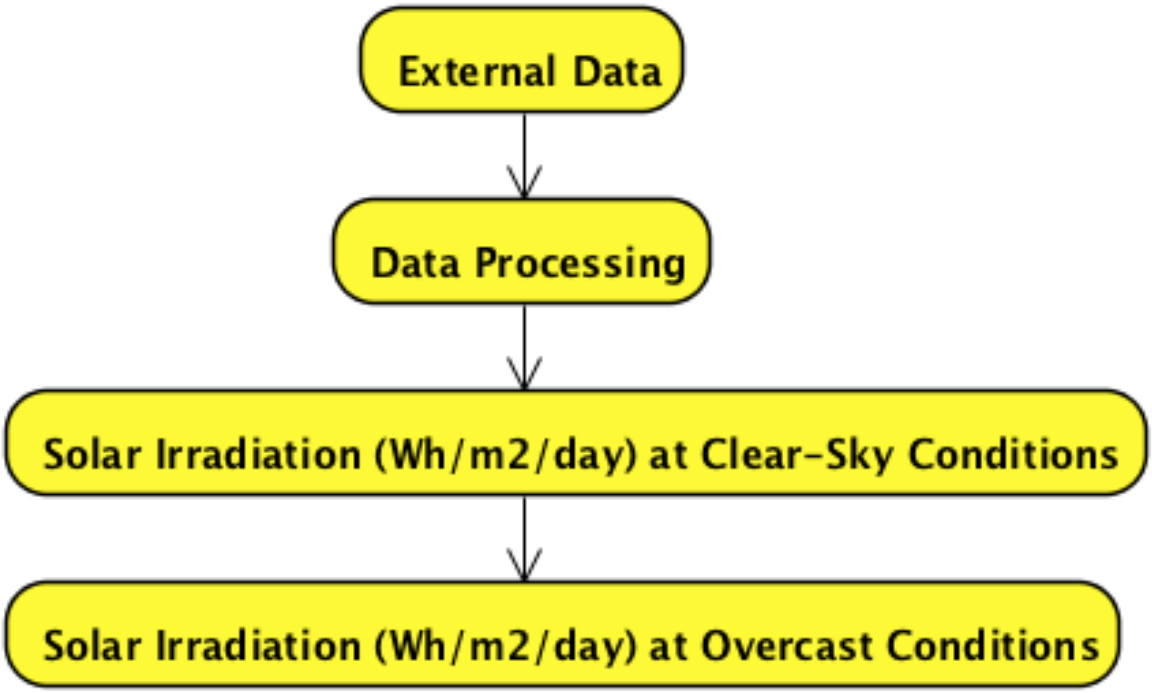

Figure 8 – The basic conceptual analysis model that is applied to the large-scale analysis.

The first component “External Data” summarizes the input data for the large-scale analysis. In that case a DEM, a shapefile that includes the study area and the albedo (parameter for the selected model) serve as input parameters. The DEM and the shapefile have to be processed before the model can be invoked. For this reason the component “Data Processing” is part of the model. For the processing of the data of the large-scale analysis merely GRASS GIS 6.4.1 is used. First, the shapefile is delineated to the study area, because it is needed to delineate the of the DEM to the study area (see Figure 9). After the shapefile is imported, the study area has to be selected and stored separately. The resulting shapefile is then converted to a raster, because GRASS GIS cannot clip a raster based on a polygon shapefile. Based on the study area raster a “mask” is defined. As long as the “mask” is active, the output of all raster operations is clipped to that area. Especially, in case of DEMs that are input and that have a larger extent than the study area, processing time can be saved.

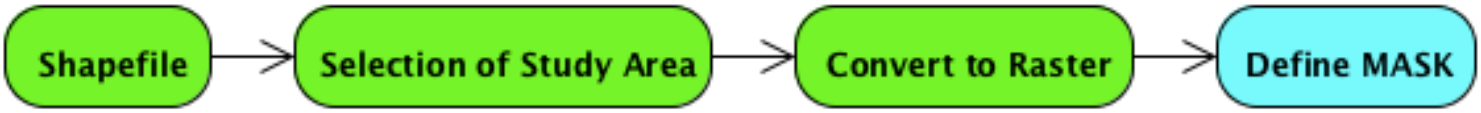

Figure 9 - Schematic representation of the workflow for defining the study area ("mask")

After the study area is defined through the "mask", the DEM processing can be started (see Figure 10). In case the extent of the DEM is smaller than the extent of the study area ("mask"), several DEMs have to be merged until the whole study area is covered. Before the slope and aspect raster are derived from the DEM, it is "cleaned". That means that all negative altitude values are replaced with value 0. The DEM, slope and aspect raster are than used as input for the model. For the processing of both workflows (see Figure 9 and 10) UNIX Shell scripts are used.

Figure 10 - Schematic representation of the workflow for the DEM processing and the creation of the slope and aspect raster.

Before the last two components are explained, a short overview about the r.sun module is given. It offers the opportunity to calculate raster maps of direct, diffuse, and reflected solar irradiation. Altogether these raster maps represent the global solar irradiation. The resulting values are daily sums of solar irradiation and given in Wh/m2/day. Parameters such as sunrise, sunset, declination, extraterrestrial irradiance or daylight length are provided by r.sun and do not have to be determined. Basically, r.sun calculates the irradiation raster for a given day, latitude, surface, and atmospheric conditions. Optionally, also the shadowing effect can be included into the calculations (Hofierka and Šúri, 2002).

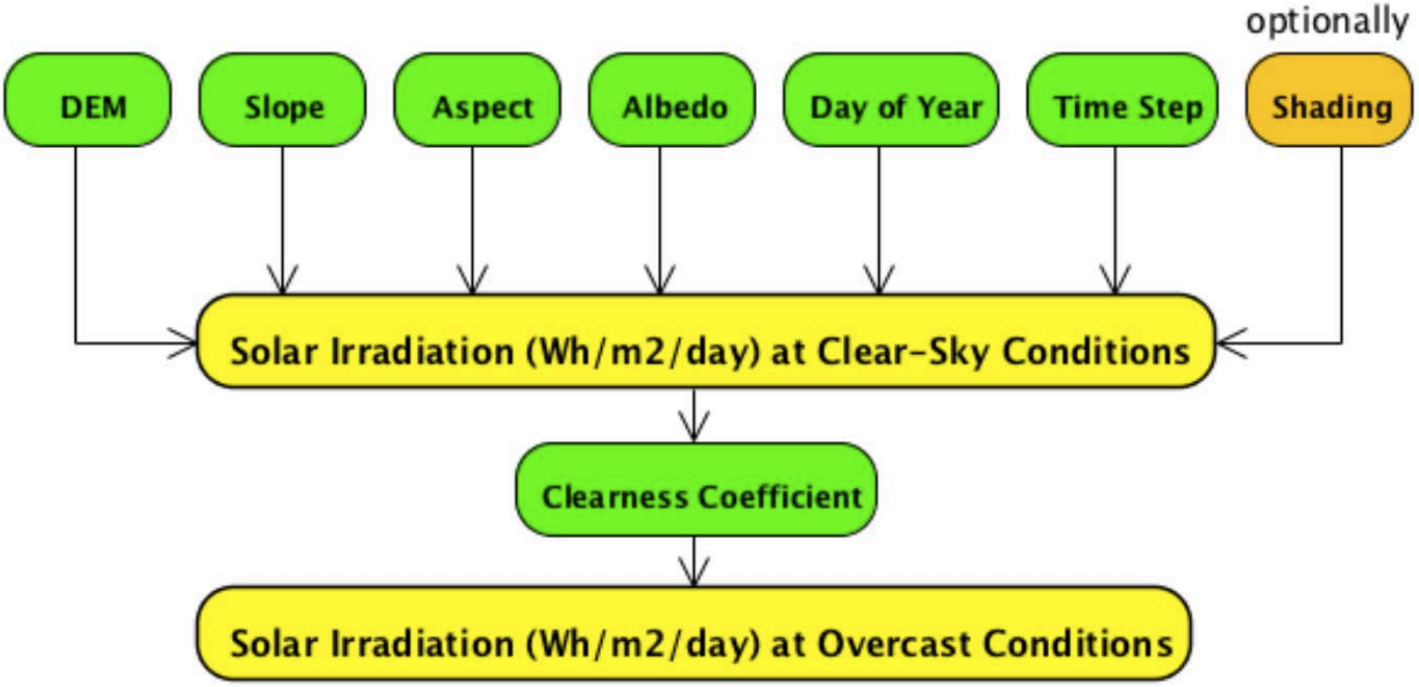

Figure 11 – Detailed representation of the selected model

In Figure 11 the last two components of the basic conceptual analysis model including the parameters to be used can be seen. As has been said before, r.sun calculates the results based on the surface, latitude, given day and atmospheric conditions. The surface is represented through the input parameters “DEM”, “Slope”, “Aspect” and “Albedo” (see Figure 11). The first three parameters are raster data sets and the last one is a single value that is determined for this specific study area (see Section 3.3). The albedo of a surface is it´s reflectance concerning solar radiation. Next, the latitude is defined by r.sun itself, based on the reference system of the input raster. r.sun calculates the results only for a single day and not for a time period. For this reason the “Day of Year” has to be set as value between 1 (January 1st) and 365 (December 31th). The “Time Step” defines the time interval for the calculation during the day. Due to the complexity of the determination of the parameters regarding atmospheric conditions (turbidity

coefficient, real-sky beam radiation coefficient, and real-sky diffuse radiation coefficient), it is decided to exclude them from the calculation using r.sun. Consequently, the output of the r.sun module represents values for clear-sky conditions. To provide values including overcast conditions, the additional parameter “Clearness Index” is added after the calculation with r.sun. The resulting raster include daily sums of global solar irradiation for a given day (Wh/m2/day) at overcast conditions, including shadowing (see Figure 11).

r.sun does not provide the possibility to calculate the incoming solar irradiation for a given time period. Within this thesis average monthly values are computed and running the module for every single day of the year separately would have cost more time than running the module for a given time period. Therefore UNIX Shell scripts are used to calculate monthly raster maps of global solar irradiation. An excerpt of the script can be seen in Figure 12. At the top (see “# 1”) the beginning of the loop can be seen. The starting and the end day have to be defined. Below (see “# 2”) the execution of the r.sun module including the input parameters is shown. Finally, (see “# 3”) the calculated values are summed up and then the loop starts again until the break condition occurs.

```
# 1
#while argument is true, do...
while [ $i -le $end ]
do
    # building the name for the maps
    DAY=`echo $i | awk '{printf("%.03d", $1)}'`
    echo "Processing day $DAY_STR at `date` ..."
# 2
    # input parameters: dem, slope, aspect, albedo (0.16), day, time step (0.5)
    r.sun -s elevin=$dem slopein=$slope aspin=$aspect alb=0.16 day=$i step=0.5\
        beam_rad=rad_beam.$DAY diff_rad=rad_diffuse.$DAY \
        refl_rad=rad_reflected.$DAY dist=0.5

# 3
    #calculate total beam irradiance
    r.mapcalc "beam_dec_$elev=beam_dec_$elev+rad_beam.$DAY"

    #calculate total diffuse irradiance
    r.mapcalc "diff_dec_$elev=diff_dec_$elev+rad_diffuse.$DAY"

    #calculate total reflected irradiance
    r.mapcalc "refl_dec_$elev=refl_dec_$elev+rad_reflected.$DAY"

    #delete created raster
    g.remove rast=rad_beam.$DAY,rad_diffuse.$DAY,rad_reflected.$DAY

    i=`expr $i + 1`
done
```

Figure 12 - An excerpt of the UNIX Shell script for the calculation of monthly values of solar irradiation.

3.4.2 Small-Scale Analysis

For the evaluation of the solar potential of roof surfaces highly accurate base data are required. For the small-scale analysis LiDAR data serve as the base data. However, the LiDAR data do not have the necessary accuracy that is stated by Klärle et al. (2009). In observance of this fact the basic conceptual analysis model of the large-scale analysis is enhanced and adapted for the small-scale analysis. The enhanced and adapted model can be seen in Figure 13 and the individual components are described below.

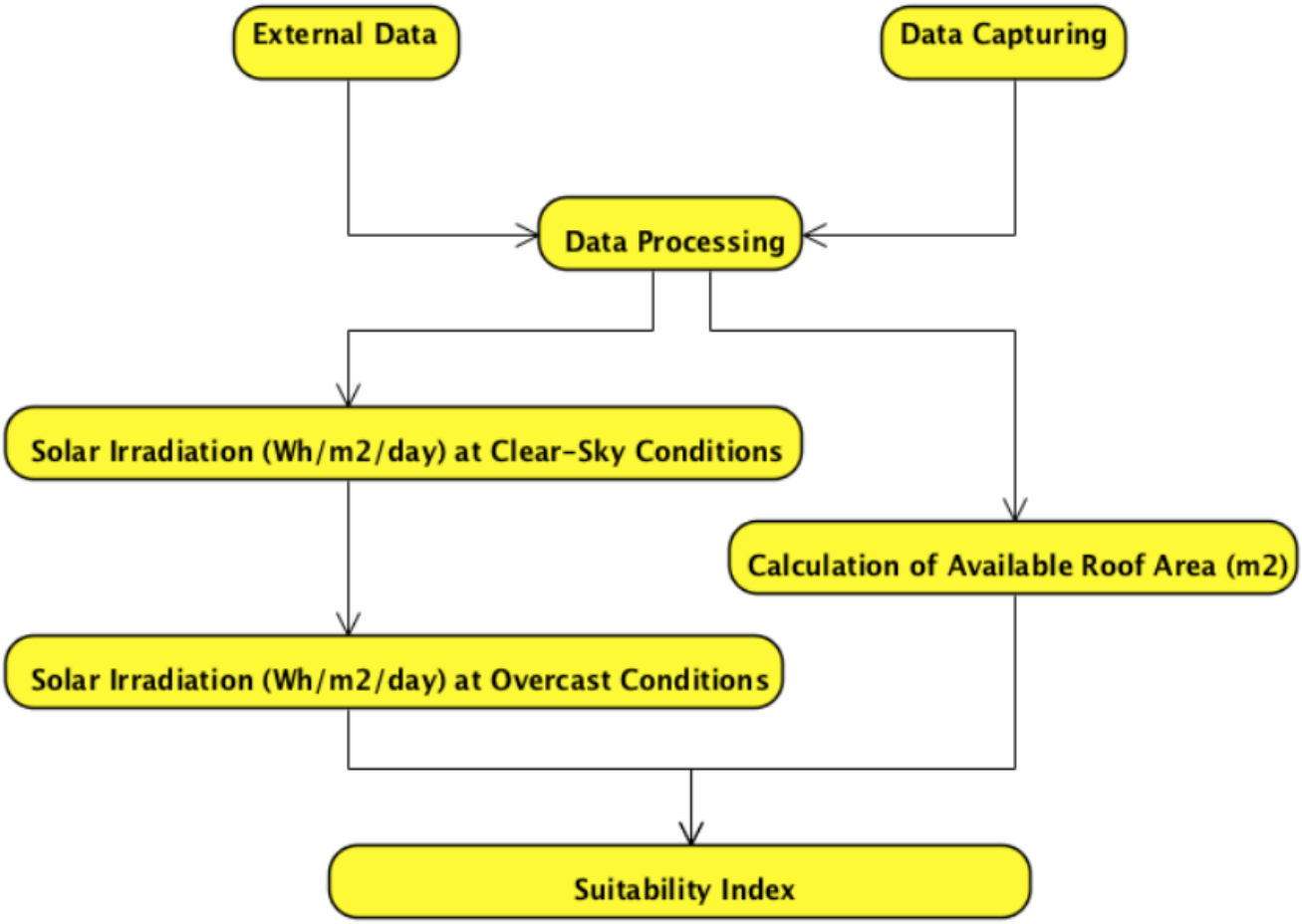

Figure 13 – Conceptual analysis model for the small-scale analysis

The component “External Data” encompasses the input data of the model. The input data are LiDAR data, a shapefile containing the building footprints of the LSU campus and the albedo. The component “Data Capturing” is added, because of the too low accuracy of the LiDAR data. Therefore additional information about the buildings is collected as described in Section 3.3 and added to the footprints attribute table. The preparation of the data for the model is again described through the component “Data Processing”. First the LiDAR data are processed to a DEM that in turn serves as input parameter for the calculation (see Fig 14). After the LiDAR data are imported into GRASS GIS they represent a point cloud of more than 3.2 millions points. To save processing time, these points are clipped to the size of the study region. For the processing of the LiDAR data to a DEM, GRASS GIS offers the

tool v.surf.rst. Based on Neteler and Mitasova (2008) a DEM is created, after testing 15 different possibilities of setting combinations. v.surf.rst offers the opportunity to output a point file that includes the deviation of the resulting surface (DEM) from the input points. Out of all DEMs the one DEM is selected that has the least average absolute deviation from the input data.

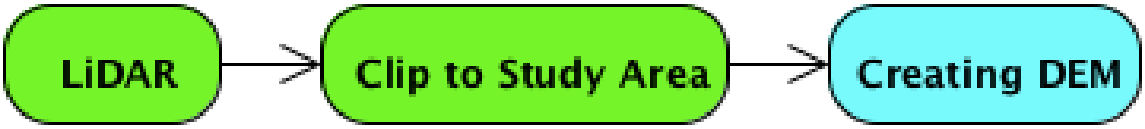

Figure 14–Schematic representation of the processing of the LiDAR data

Another consequence of the too low accurate LiDAR data is that the slope and aspect raster cannot be derived from the DEM, because it cannot be assumed that the DEM is accurate enough for this type of analysis. For this reason the two raster are derived through converting the building footprints to a raster, based on the selected information about slope and aspect. These two raster are then used as input for the calculation. The model follows the same procedure as previously described in Section 3.4.1, except that shadowing is not included. Shadowing has a strong influence on the results of the calculation model and for the same reason as for slope and aspect it cannot be derived from the input data. Manually modeling and determining the influence of shadowing is out of the scope of this research.

Another component deals with the calculation of the available roof surface. The calculation of the roof surface is based on the area of the building footprints. As described in Section 3.3the buildings can be divided into several surfaces. In those cases the incoming solar irradiation and the available roof surface is calculated for each individual sub-surface and summed up afterwards. The available roof surface is calculated based on the manually collected roof type- and facility coefficient by multiplying it with the size of the surface or footprint area. Having a building

footprint area of 100 m^2, a roof type coefficient of 0.5 and a facility coefficient of 0.9 would result in an available roof area of 45 m^2.

The available roof area and the calculated incoming solar irradiation at overcast conditions are then manually combined and averaged. In addition total daily and yearly values of incoming solar irradiation per building are calculated. The suitability of the roof surfaces is then described through the "Suitability Index". This index is divided into three categories (unsuitable, well suited, and very well suited) and applied to the study area.

3.5 Summary

At the beginning the Section "Methodology" summarized the multiple challenges of this thesis. Subsequently, the two study areas and why they were selected are described. The description of the two study areas is followed by a detailed discussion of the data to be used in this research. Especially, the different projections and data types are emphasized. Finally, the Section "Method of Solution" presents solutions to the defined problem. It includes the reasons why this particular GIS is chosen for this research. Furthermore, the development of the conceptual analysis model is described in detail. Also the application of UNIX Shell scripts, to support a semi-automated data processing, is mentioned.

4. Results and Interpretation

In this Section the results of this research are presented and discussed. First the results of the large-scale analysis are delineated, comparing the results of the model with the reference values for East Baton Rouge Parish. Then the results of the small-scale analysis are described, where selected rooftops of the LSU main campus are evaluated on their potential for collecting solar power.

4.1 Large-Scale Analysis

The main reason to perform the large-scale analysis is to evaluate the results of the chosen and adapted model for this research. Furthermore, the influence of the MAUP on the results is tested. This Sub-Section summarizes the results of the large-scale analysis and provides an interpretation of them.

Based on four different DEM resolutions (1 km, 90 m, 30 m, 5m) monthly and yearly values of incoming solar irradiation per square meter (kWh/m^2) are calculated for the area of East Baton Rouge Parish. Shadowing is included into the calculations. For the evaluation of the model results, reference values from NREL 2 (n.d.) and Gaisma (2002) are applied. An overview about the reference values, the clearness index and the calculated results can be seen in Table 4. The clearness index is a parameter that is applied to the results of the r.sun module that accounts for overcast conditions.

Table 4–Overview of the reference values (1 and 2) (kWh/m^2), clearness index (3) and the results (4-7) (kWh/m^2) that are calculated in this research.
(1 = NREL 2 (n.d.), 2 = Gaisma (2002), 3 = NREL 1 (n.d.), 4 = DEM 1km (GTOPO 30, 1996), 5 = DEM 30m (Jarvis et al., 2008), 6 = DEM 30m (USGS, 2009), 7 = DEM 5m (USACE 1, 2001).

	jan	feb	mar	apr	may	jun	jul	aug	sep	oct	nov	dec	year
1	2.60	3,50	4.40	5.40	5.90	6.00	5.70	5.40	4.80	4.30	3.00	2.50	4.46
2	2.58	3.26	4.38	5.35	5.83	5.62	5.62	5.27	4.88	4.08	3.03	2.43	4.36
3	0.45	0.48	0.50	0.52	0.53	0.53	0.51	0.51	0.51	0.55	0.48	0.48	0.45
4	2.59	3.39	4.34	5.26	5.82	5.99	5.66	5.29	4.67	4.17	2.92	2.41	4.37
5	2.59	3.39	4.34	5.26	5.82	5.98	5.66	5.29	4.67	4.17	2.93	2.41	4.38
6	2.58	3.38	4.34	5.26	5.82	5.99	5.66	5.29	4.67	4.16	2.92	2.40	4.37
7	2.60	3.39	4.35	5.26	5.82	5.98	5.65	5.29	4.67	4.17	2.93	2.42	4.38

Based on the principle of the MAUP, which implies that results based on the same spatial area can differ from each other when different LoDs are used, it was assumed that the results of the different LoDs applied in this research would greatly vary. When looking at the results of the calculated average yearly values of incoming solar irradiation, it can be seen that surprisingly, the results are rather similar to each other (4.37 – 4.38 kWh/m^2) (see Table 4). Consequently, there does not seem to be too much influence of the MAUP on the results of this large-scale analysis. It is believed that the MAUP is inefficacious in this type of analysis, because of the flat topographic profile of the East Baton Rouge Parish. Most slope values are in the range between 0 and 20°. Only occasionally can slope values higher than 20° be found.

As can also be seen in Table 4 the calculated values of monthly and yearly incoming solar irradiation are only slightly different from the reference values. Either the calculated values are in the range of the two reference values or they are slightly lower than the reference values. Among the calculated values the maximum differences between the values are 0.02 kWh/m^2. Figure 15 shows a chart that represents the variation of the calculated irradiation values of the 5m DEM during

the course of one year. The trend of the values closely follows the shape of a parabola, having its peak in June with an incoming solar irradiation of 5.98 kWh/m^2.The value in December is about 40.47% of the peak value. From March to October the irradiation values are always above 4 kWh/m^2. Adding up all twelve monthly values an average yearly irradiation value of 1598.7 kWh/m^2 is calculated. Considering that the study area has an area of 1220 km^2 (471 square miles), the total incoming irradiation per year is about 1950.414 GWh. When comparing the irradiation values of the East Baton Rouge Parish, yearly irradiation values for Germany are about 1100 kWh/m^2 and in Chile the highest values are about 2800 kWh/m^2 (Klärle et al., 2009). It can be seen that the solar potential in East Baton Rouge Parish is higher than in Germany, but somewhat lower than the solar potential in Chile.

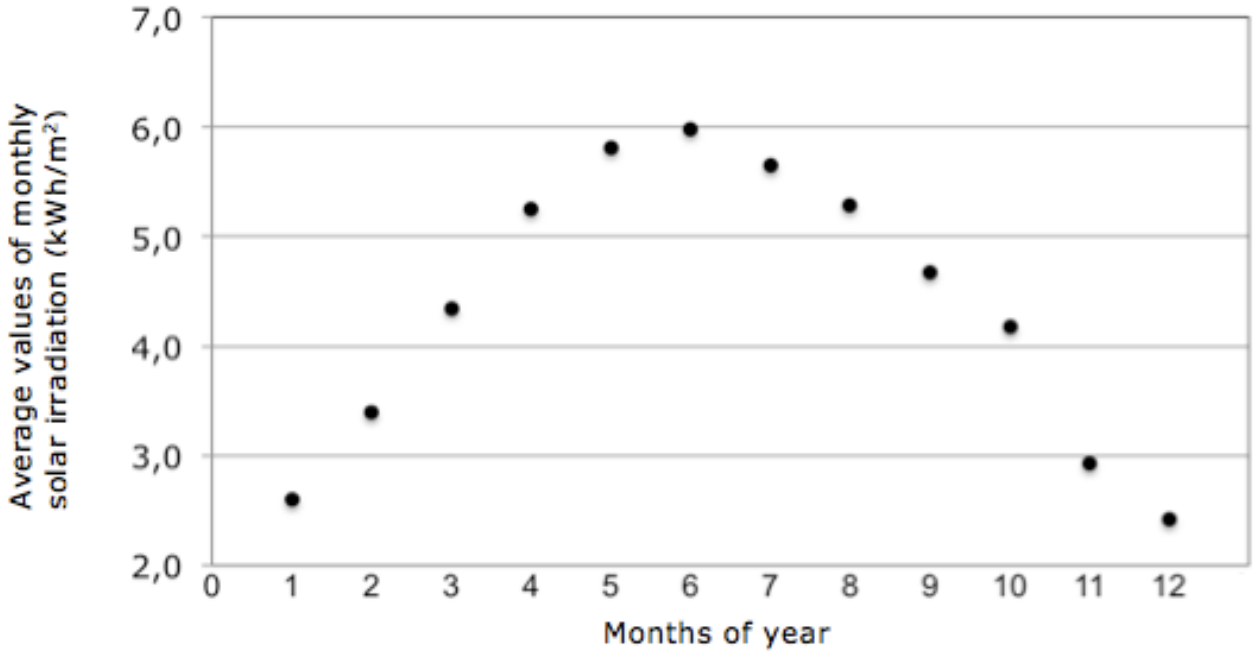

Figure 15– The variation of the solar irradiation of the 5m DEM during the course of the year

Due to the closeness of the calculated irradiation values to the reference values, it is believed that the calculation model of this research is capable of producing somewhat accurate results. It has to be considered that the study area has a flat topographic profile. When using the same model for mountainous regions, the influence of the topography on the results has to be addressed and evaluated.

4.2 Small-Scale Analysis

In order to increase the likelihood of Baton Rouge inhabitants to install solar panels on their homes, the small-scale analysis is performed for 50 selected roof surfaces (see Figure 16 – yellow building footprints) of the LSU main campus. Based on LiDAR data, the building footprints, and additionally collected information about the roof surfaces (roof type, roof type coefficient, and facility coefficient), the small-scale analysis is implemented. In this Sub-Section the results of the solar potential analysis of the roof surfaces are presented and discussed.

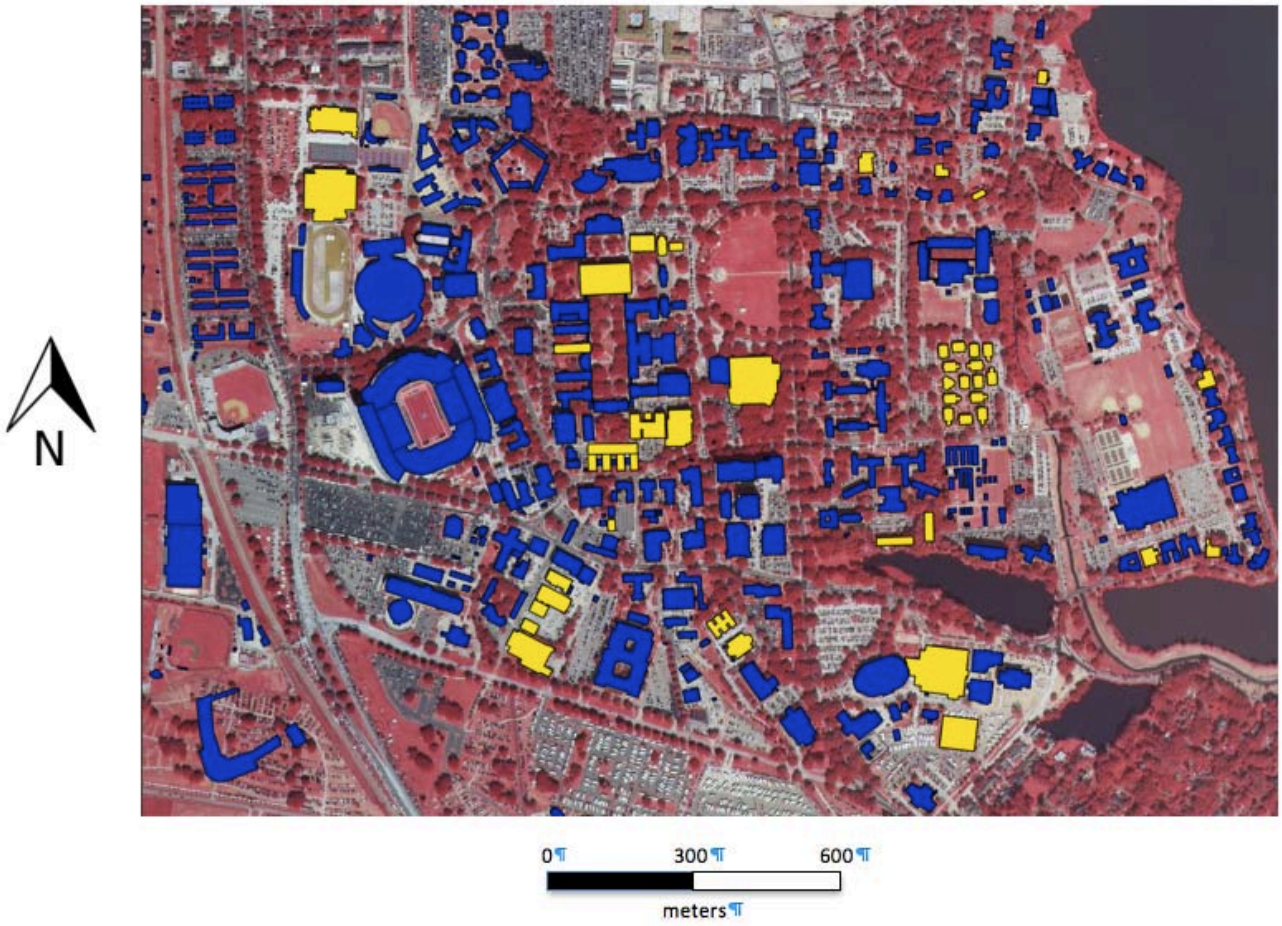

Figure 16 - The selected buildings for the small-scale analysis can be seen in yellow.

For the 50 selected buildings, a total of 68 roof surfaces are collected and rated for this analysis. Complex roof surfaces were divided into multiple sub-surfaces, resulting in 68 roof (sub) surfaces from the original 50 buildings. In total 13 roof surfaces are rated as “flat”, 21 as “gabled” and 34 as “other”. For the “other” category, the entire roof surface was further divided into sub-surfaces. The areas of the roof surfaces are calculated based on the building footprints. The 50 selected buildings have a total roof surface area of 104,492.2 m^2. This represents about 18.16% of the total roof surface area of the LSU main campus (574,998.9 m^2). After categorizing the roof surfaces and when considering that not the total roof surface area can be used for installing solar panels, a total roof surface area of 58,944.6 m^2 (10.25%) is used as being suitable for installing solar panels.

In Figure 17 the result of the small-scale analysis can be seen. The roof surfaces of the 50 buildings are rated according to the categories of the suitability index. In addition the corresponding irradiation values are shown. Due to the high solar potential of the study area – the average incoming solar irradiation per year is about 40% higher than the peak value in Germany - the suitability index is formed using the classification method “Jenks Natural Breaks”. 4 buildings of the study area are classified as “unsuitable”, because of the orientation of their roof surface. 28 buildings are classified as “well suited” (4.2 – 4.63 kWh/m^2/day) and the remaining 18 buildings as “very well suited” (4.64 – 4.96 kWh/m^2/day).

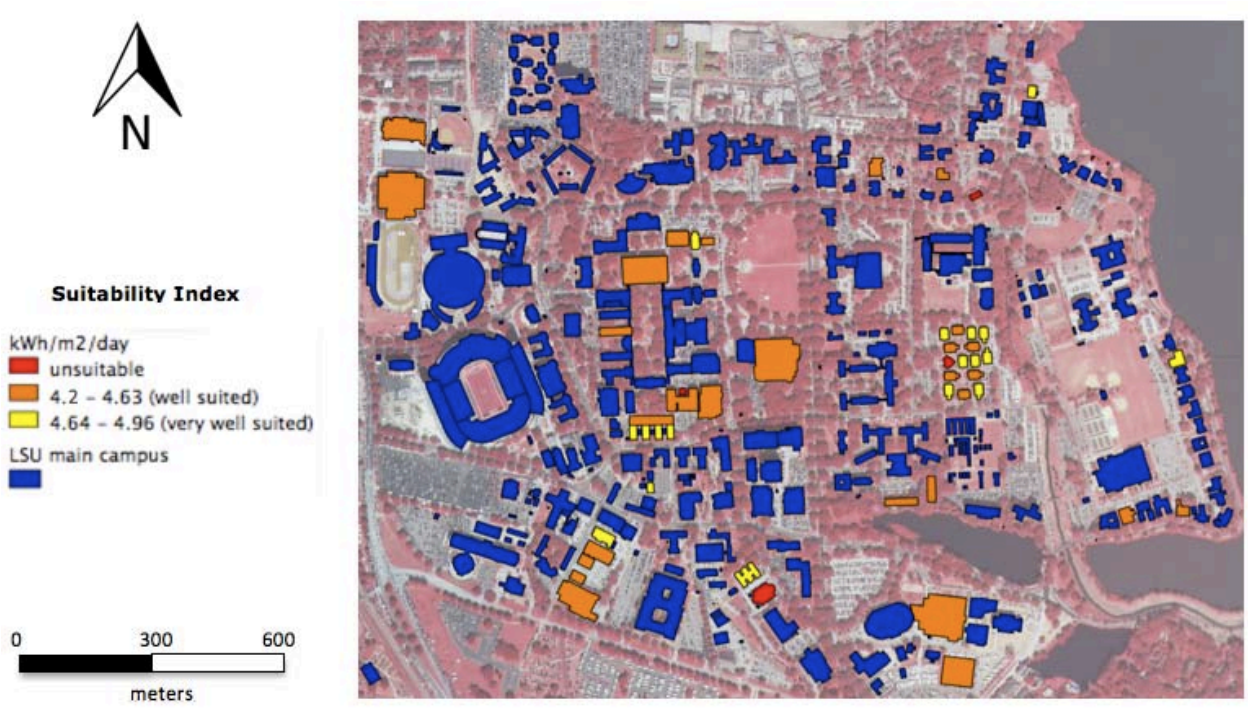

Figure 17 - Result of the small-scale analysis.

For all selected buildings the average incoming solar irradiation is about 4.22 kWh/m^2/day or 1540.3 kWh/m^2/year. Excluding the “unsuitable” buildings results in an average value of 4.58 kWh/m^2/day or 1671.7 kWh/m^2/year. Finally, after the

incoming irradiation is calculated for each building, the possible energy output is calculated. Based on the work of Wiginton et al. (2010), two types of solar panels are applied to the estimation of the energy output. The two types are crystalline silicon- [Si(crystalline)] and multi-crystalline silicon [Si(multicrystalline)] solar panels. The first type has a module efficiency of 22.9% and the second of 15.5%. Table 5 gives an overview about the power and energy output for these two types of solar panels. In addition, the potential saving in US Dollar for the two types is included. The potential savings are calculated using the average electricity price of the state of Louisiana, based on a value of 7.16¢/kWh(IER, 2010).Looking at the results of the crystalline silicon solar panel, it can be seen that throughout the year 20,776,630.34 kWh could be produced, if this type of solar panel is installed on the suitable roof surfaces. Consequently, $1.5 million on energy costs could be saved every year. In contrast, when installing the multi-crystalline silicon solar panels that have a lower efficiency, 14062784.73 kWh can be produced, resulting in potential savings of $1 million. When thinking about the fact that the analysis of this research is made for 18.16% of the total roof surface area of the LSU main campus, the potential savings per year could be approximately 5 times higher. This would result in potential savings of $7.5 [Si(crystalline)] or $5 [Si(multicrystalline)] million a year. The purchase, the installation, and the maintenance of the solar panels are not included in the estimations made in this research.

Table 5 – Power and energy output based on two different types of solar panels. Additionally, the potential savings per year are included.

Panel Type	Module Efficiency	Panel output ($kWh/m^2/day$)	Annual panel output (kWh/m^2)	Annual panel output for all buildings (kWh)	Potential savings per year in $
Si(crystalline)	22.9%	0,97	352.5	20776630.34	1487607
Si(multicrystalline)	15.5%	0.54	238.6	14062784.73	1006895

It has to be considered that the results of the small-scale analysis include instability factors. The calculation model is tested for an area that has a flat topographic profile. The small-scale analysis includes roof-surfaces that have slope values up to 30°. Furthermore, shadowing is not accounted for in this model or in the results. Therefore, the estimated results of the small-scale analysis have to be further refined. Moreover, the calculation of the roof surface areas has to be reconsidered. The calculation is based on the flat building footprints and the inclination of the roof surfaces is not accounted for in the calculation of the roof surface areas. The integration of the inclination is thus another important factor that has to be considered in the future.

5. Discussion

The hypothesis that was stated at the beginning of this research (see Section 1.4) is discussed in this Section. Furthermore, the expected results (see Sections 1.3) are compared with the actual outcome of this research.

The hypothesis stated that the application of GIS integrated calculation models enables the accurate estimations of incoming solar irradiation. During the course of this research this assumption was validated for areas having a flat topographic profile. The results have shown that the applied model is capable of producing accurate results. Nevertheless, the results of the model for areas having a varied topographic profile (inclined surfaces) have not yet been tested or evaluated. The additional assumption that GISs enable the aggregation of irradiation values on pre-defined surfaces can be confirmed. The results of incoming solar irradiation were aggregated based on the building footprints of the main campus of the LSU. This made the calculation of incoming solar irradiation for each building possible.

Most of the initially set expectations of this research have been met. As it was expected at the beginning of this research a conceptual analysis model for the estimation of the solar potential of roof surfaces has been developed. Unfortunately, the evaluation of the geodata on their “fitness for use” has shown that the accuracy of the LiDAR data was not as accurate as expected. At the beginning it was believed that the DEM, slope and aspect could be generated based on the LiDAR data. Due to the low accuracy of the LiDAR data only the DEM was created based on these data. Slope and aspect were manually determined and integrated. Based on the given data basis the conceptual analysis model has been implemented using GRASS GIS 6.4.1. As it was anticipated the results are described using the suitability index. In addition to the expected results, a prediction of potential savings in energy costs was also provided.

6. Summary

This Section summarizes the work that has been done during this thesis research and provides an overview about aspects and ideas that can be considered and implemented in the future.

6.1 Conclusion

It can be summarized that in the course of this research a conceptual analysis model for the estimation of the solar potential of roof surfaces has been developed. The development process included the evaluation of the selected model, based on the area of East Baton Rouge Parish. It has been shown that the calculated results are within the range of the reference values. Because the available LiDAR data were not accurate enough for estimating roof surface areas, additional information concerning the roof surfaces (roof type, roof type- and facility coefficient, slope and aspect) had to be collected and included into the analysis. To speed up the processing of the data, workflows were created and implemented using UNIX Shell scripts. The using of scripts enabled a semi-automated processing of the data. The analysis results showed that the yearly solar irradiation of the entire East Baton Rouge Parish is about 1598.7 kWh/m^2 or 1950.414 GWh. In comparison, in Germany yearly irradiation values of 1100 kWh/m^2 have been calculated. This represents 68.8% of the solar potential of the East Baton Rouge Parish. For the solar potential analysis of the roof surfaces 50 buildings of the LSU main campus were selected. They represent 18.6% of the total roof surface area. The results of the roof top analysis are described by the suitability index that is classified into three categories (unsuitable, well suited, and very well suited). The average incoming solar irradiation of the roof surfaces is 4.22 kWh/m^2/day or 1540.3 kWh/m^2/year. It has to be noted that the roof surface area of the “unsuitable”

ranked buildings is included into the calculation of these values. Based on the use of two different types of solar panels, yearly savings in energy costs were estimated. Depending on the panel type, savings of $1 - $1.5 million are possible for each year for the selected buildings. For the whole LSU main campus potential savings of $5 – $7.5 million can thus be achieved. The purchase, the installation, and the maintenance of the solar panels is not included into the estimations. It has to be noted that shadowing is not included into the model and the analysis. If shadowing is present, it has a negative influence on the output of the solar panels. Furthermore, the calculation model is tested for a flat topographic profile. The influence of inclined surfaces on the results has not been tested yet.

6.2 Future Perspectives

The current version of the conceptual analysis model enables the estimation of the solar potential of roof surfaces. The calculations are based on a calculation model that has been evaluated for an area having a flat topographic profile. Due to the existing inclination of the roof surfaces, the results of the calculations also have to be verified and evaluated for these conditions.

Another aspect that has to be considered in future research is shadowing. Shadowing has a negative influence on the total amount of energy produced by solar panels. It was not possible to determine the shadowing influence of objects such as trees or chimneys, because the base data were not enough accurate.

Furthermore, the calculation of the available roof surface area has to be improved. Currently, it is calculated based on the flat building footprints. The incorporation of the inclination of the roof surfaces into the estimation of their area would increase the accuracy of this research.

Finally, the expansion of this analysis to the entire LSU campus and the representation of the results within a publicly available Web GIS are other aspects that can be considered in the future.

7. References

Cebecauer, T., Huld, T., Šúri, M., 2007.Using high-resolution digital elevation model for improved PV yield estimates, *Proceedings of the 22nd European Photovoltaic Solar Energy Conference*, 3553-3557.

Chrysoulakis, N., Diamantakis, M., Prastacos, P., 2004. GIS based estimation and mapping of local level of daily irradiation on inclined surfaces, *Proceedings of the 7th AGILE Conference on Geographic Information Science*, 587 – 597.

Compagnon, R., 2004. Solar and daylight availability in the urban fabric, *Energy and Buildings*, 36 (4), 321-328.

Conrad, O., 2001. *SAGA GIS Module: Incoming Solar Radiation* [online]. Available from:*http://www.saga-gis.org/saga_modules_doc/ta_lighting/ta_lighting_02.html* [Accessed 15 April 2011].

Conrad, O., 2006. SAGA GIS Module: Insolation [online]. Available from:*http://www.saga-gis.org/saga_modules_doc/ta_lighting/ta_lighting_03.html* [Accessed 15 April 2011].

Environmental Systems Research Institute (ESRI), 2006. ArcGIS Tool: Area Solar Radiation [online]. Available from: *http://webhelp.esri.com/arcgiSDEsktop/9.3/index.cfm?TopicName=Area_Solar_Radiation* [Accessed 15 April 2011].

Environmental Systems Research Institute (ESRI), 2011.ArcGIS Desktop [online]. Available from: *http://www.esri.com/software/arcgis/* [Accessed 15 April 2011].

FEMA, 2003**.** *Guidelines and Specifications for Flood Hazard Mapping Partners* [online],Federal Emergency Management Agency. Available from: *http://www.fema.gov/library/viewRecord.do?id=2206* [Accessed 15 April 2011].

Fthenakis, V., Mason, J. E., Zweibel, K., 2009. The technical, geographical, and economic feasibility for solar energy to supply the energy needs of the US. *Energy Policy*, 37 (2), 387-399.

Gaisma, 2002. *Solar energy and surface meteorology* [online].Available from:*http://www.gaisma.com/en/location/baton-rouge-louisiana.html* [Accessed 15 April 2011].

Governor's Office of Homeland Security and Emergency Preparedness (GOHSEP), n.d.. *LA Earth client* [online]. Available from: *http://www.gohsep.la.gov/laearth.aspx* [Accessed 15 April 2011].

GRASS Development Team, 2011. Available from: http://grass.osgeo.org [Accessed 15 April 2011].

Global 30 Arc-Second Elevation Data Set (GTOPO30), 1996. *Global 30 Arc-Second Elevation (GTOPO 30)* [online].EROS Data Center (EDC) Distributed Active Archive Center (DAAC), Sioux Falls, South Dakota, USA. Available from: *http://eros.usgs.gov/#/Find_Data/Products_and_Data_Available/gtopo30_info* [Accessed 15 April 2011].

Hartmann, N., Glueck, C., Schmidt, F. P., 2011. Solar cooling for small office buildings: Comparison of solar thermal and photovoltaic options for two different European climates. *Renewable Energy*, 36(5), 1329-1338.

Herbst, D., 2009. Solar mapping: demystifying solar potential. *Renewable Energy Focus*, 10(4), 32-35.

Hofierka, J., Kanuk, J., 2009. Assessment of photovoltaic potential in urban areas using open-source solar radiation tools. *Renewable Energy*, 34 (10), 2206-2214.

Hofierka, J. and Šúri, M., 2002. *GRASS GIS module: r.sun* [online]. Available from: *http://grass.fbk.eu/grass62/manuals/html62_user/r.sun.html* [Accessed 15 April 2011].

Huld, T. A., Šúri, M., Dunlop, E. D., 2003.GIS-based Estimation of Solar Radiation and PV Generation in Central and Eastern Europe on the Web, *9th EC-GI&GIS Workshop*, Coruña, Spain.

IEA/SHC Task 36, 2010. Available from: *http://www.iea-shc.org/task36/* [Accessed 15 April 2011].

Institute for Energy Research (IER), 2010. *Louisiana Energy Facts* [online]. Available from: http://www.instituteforenergyresearch.org/state-regs/pdf/Louisiana.pdf [Accessed 25 April 2011].

Izquierdo, S., Rodrigues, M., Fueyo, N., 2008. A method for estimating the geographical distribution of the available roof surface area for large-scale photovoltaic energy-potential evaluations. *Solar Energy*, 82 (10), 929-939.

Izquierdo, S., Dopazo, C., Fueyo, N., 2010. Supply-cost curves for geographically distributed renewable-energy resources. *Energy Policy*, 38 (1), 667-672.

Izquierdo, S., Montanes, C., Dopazo, C., Fueyo, N., 2011. Roof-top solar energy potential under performance-based building energy codes: The case of Spain. *Solar Energy*, 85 (1), 208-213.

Jarvis, A., Reuter, H.I., Nelson, A., Guevara, E., 2008. *Hole-filled seamless SRTM data V4* [online]. International Centre for Tropical Agriculture (CIAT). Available from: *http://srtm.csi.cgiar.org* [Accessed 15 April 2011].

Jelinski, D. and Wu, J., 1996. The modifiable areal unit problem and implications for landscape ecology. *Landscape Ecology*, 11 (3), 129-140.

Juanico, L., 2008. A new design of roof-integrated water solar collector for domestic heating and cooling. *Solar Energy*, 82 (6), 481-492.

Klärle, M., Lanig, S., Ludwig, D., 2009. Towards Location-based Analysis for Solar Panels by High Resolution Remote Sensors (Laser Scanner). *24th International Cartography Conference. Santiago*, Chile,43.

Kovach, A. and Schmid, J., 1996. Determination of energy output losses due to shading of building-integrated photovoltaic arrays using a ray tracing technique. *Solar Energy*, 57 (2), 117-124.

Lehmann, H. and Peter, S.,2003. Assessment of roof & façade potentials for solar use in Europe. *Institute for sustainable solutions and innovations (ISUSI)*, Aachen, Germany.

Levinson, R., Akbari, H., Pomerantz, M., Gupta S., 2009. Solar access of residential rooftops in four California cities. *Solar Energy*, 83 (12), 2120-2135.

Louisiana Department of Transportation and Development (LDOTD), 2007. *Louisiana Parish Boundaries*[online]. Available from: *http://lagic.lsu.edu/data/losco/parishes_ldotd_2007_faq.html* [Accessed 15 April 2011].

LSU CADGIS Research Laboratory, 2009. *Atlas: The Louisiana Statewide GIS* [online], LSU CADGIS Research Laboratory. Available from: *http://atlas.lsu.edu* [Accessed 15 April 2011].

Mellit, A., Kalogirou, S.A., Shaari, S., Salhi, H., Arab, A., 2007. Methodology for predicting sequences of mean monthly clearness index and daily solar radiation data in remote areas: Application for sizing a stand-alone PV system. *Renewable Energy*, 33 (7), 1570-1590.

Maneewan, S., Hirunlabh, J., Khedari, J., Zeghmati, B., Teekasap, S., 2005. Heat gain reduction by means of thermoelectric roof solar collector. *Solar Energy*, 78 (4), 495-503.

Mesor, 2011. Available from: *http://www.mesor.org/home.html* [Accessed 15 April 2011].

National Renewable Energy Laboratory (NREL) 1, n.d.. Available from:

http://rredc.nrel.gov/solar/old_data/nsrdb/1961-1990/bluebook/state.html [Accessed 15 April 2011].

National Renewable Energy Laboratory (NREL) 2, n.d.. Available from: *http://rredc.nrel.gov/solar/old_data/nsrdb/1961-1990/redbook/sum2/state.html* [Accessed 15 April 2011].

Neteler, M. and Mitasova H., 2008. *Open Source GIS - A GRASS GIS Approach (Third Edition)*, New York: Springer.

Noorian, A. M., Moradi, I., Kamali, G. A., 2008. Evaluation of 12 models to estimate hourly diffuse irradiation on inclined surfaces. *Renewable Energy*, 33 (6), 1406-1412.

Nguyen, H. T. and Pearce, J.M., 2010. Estimating Potential Photovoltaic Yield with r.sun and the Open Source Geographical Resources Analysis Support System. *Solar Energy*, 84 (5), 831-843.

Pandey, C. K. and Katiyar A.K., 2011. A comparative study of solar irradiation models on various inclined surfaces for India. *Applied Energy*, 88 (4), 1455-1459.

Parida, B., Iniyan, S., Goic, R., 2011. A review of solar photovoltaic technologies. *Renewable and Sustainable Energy Reviews,* 15 (3), 1625-1636.

Perez, R., Ineichen, P., Seals, R., 1990. Modeling daylight availability and irradiance components from direct and global irradiance. *Solar Energy*, 44(59), 271–89.

Quantum GIS (QGIS) Development Team, 2011. Available from: *http://qgis.osgeo.org* [Accessed 15 April 2011].

Quaschning, V. and Hanitsch R., 1998. Irradiance calculation on shaded surfaces. *Solar Energy*, 62 (5), 369-375.

Ramachandra, T.V. and Shruthi, B.V., 2007. Spatial mapping of renewable energy potential. *Renewable and Sustainable Energy Reviews*, 11 (7), 1460-1480.

Rylatt, M., Gadsden, S., Lomas, K., 2001. GIS-based decision support for solar energy planning in urban environments. *Computers, Environment and Urban Systems*, 25 (6), 579-603.

SAGA Development Team, 2011. Available from: http://www.saga-gis.org/ [Accessed 15 April 2011].

San Francisco Solar Map, 2007. Available from: *http://sf.solarmap.org/* [Accessed 15 April 2011].

SBDART MatLab Tool, 2011. Available from: *http://www.paulschou.com/tools/sbdart/matlab.php* [Accessed 15 April 2011].

SBDART Web Tool, 2011. Available from: *http://www.paulschou.com/tools/sbdart/* [Accessed 15 April 2011].

Sharma, A., 2011. A comprehensive study of solar power in India and World. *Renewable and Sustainable Energy Reviews*, 15 (4), 1767-1776.

Skartveit, A. and Olseth, J. A., 1986.Modelling slope irradiance at high latitudes. *Solar Energy*, 36 (4), 333–344.

Solar Boston Interactive GIS Map, 2007. Available from: *http://gis.cityofboston.gov/solarboston/* [Accessed 15 April 2011].

Soule, R., Meyers, C., Rinaudo, J., Laffoon, C., Dorris, S., Madura, R. L., Tober, L., Pakunpanya, S. P., Group, LLC, 2006. Available from: *http://www.google.com/url?sa=t&source=web&cd=1&ved=0CBcQFjAA&url=http%3A%2F%2Ftrinityconsultants.com%2FWorkArea%2FDownloadAsset.aspx%3Fid=1647&ei=X8uoTbDoIsu4twf16aXdBw&usg=AFQjCNFzRLzNNiFg5RzPDqJbzoag6jesQw* [Accessed 15 April 2011].

Šúri, M. and Hofierka, J., 2004. A New GIS-based Solar Radiation Model and Its Application to Photovoltaic Assessments. *Transactions in GIS*, 8(2), 175–190.

U. S. Army Corps of Engineers (USACE) - Saint Louis District 1, 2001. *Digital Elevation Model (USGS DEM), wx quadrant of yz quadrangle, Louisiana, UTM 15 NAD83, Louisiana FEMA Project - Phase 1: Amite River Basin, USACE (2001)* [online]. *Available from: http://atlas.lsu.edu/lidar/* [Accessed 15 April 2011].

U.S. Army Corps of Engineers (USACE) - Saint Louis District 2, 2001. *Raw LIDAR Elevation Data, NW quadrant of Baton Rouge West quadrangle, Louisiana, UTM 15 NAD83, Louisiana FEMA Project - Phase 1: Point Coupee, USACE (2001)*[online]. *Available from : http://atlas.lsu.edu/lidar/* [Accessed 15 April 2011].

U.S. Census Bureau, 2010. *State & county Quickfacts: East Baton Rouge Parish* [online]. *Available from: http://quickfacts.census.gov* [Accessed 15 April 2011].

U.S. Energy Information Administration (EIA), 2011. Available from: *http://www.eia.gov/todayinenergy/detail.cfm?id=310* [Accessed 15 April 2011].

U.S. Energy Information Administration (EIA), 2010. *Renewable Energy Annual 2008* [online]. Available from: *http://www.eia.gov/cneaf/solar.renewables/page/rea_data/rea.pdf* [Accessed 15 April 2011].

U.S. Geological Survey (USGS), 2004. *Baton Rouge West, LA SE USGS DOQQ* [online]. Available from: *http://atlas.lsu.edu/doqq2004/* [Accessed 15 April 2011].

U.S. Geological Survey (USGS), 2009. *1-Arc Second National Elevation Dataset* [online]. Available from: *http://www.truflite.com/workshop/SRTM/text/import.htm* [Accessed 15 April 2011].

Weiss, W. and Mauthner, F., 2010. Solar Heat Worldwide – Markets and Contribution to the Energy Supply 2008 [online]. Institute for Sustainable Technologies. Available from: *http://www.iea-shc.org/publications/downloads/Solar_Heat_Worldwide-2010.pdf* [Accessed 15 April 2011].

Wiginton, L.K., Nguyen, H.T., Pearce, J.M., 2010. Quantifying rooftop solar photovoltaic potential for regional renewable energy policy. *Computers, Environment and Urban Systems*, 34 (4), 345-357.

8. List of Figures

9. List of Tables